UNIVERSITY OF CALIFORNIA, SAN DIEGO

MECHANISMS OF POST-MYOCARDIAL INFARCTION HEALING: FROM ACUTE SURVIVAL TO CHRONIC REMODELING

A dissertation submitted in partial satisfaction of the requirements
for the degree Doctor of Philosophy
in Bioengineering

by

Darlene L. Hunt

Committee in charge:

Professor Andrew D. McCulloch, Chair
Professor Jeffrey H. Omens, Co-Chair
Professor Robert S. Ross
Professor Robert L. Sah
Professor Francisco J. Villarreal

2009

The dissertation of Darlene L. Hunt is approved, and it is acceptable in quality and form for publication on microfilm and electronically:

_____

_____

_____

_____
Co-Chair

_____
Chair

University of California, San Diego

2009

TABLE OF CONTENTS

LIST OF FIGURES

LIST OF TABLES

ACKNOWLEDGEMENTS

The work presented in this dissertation represents about four of the last five years I have been a part of the Cardiac Mechanics Research Group as a graduate student in the Bioengineering department at UCSD. Since arriving in San Diego in 1999 as an undergraduate freshman, I have witnessed the department grow from cramped quarters in EBU I to a brand-new building (with windows in all the labs!) by the time I graduated with a BS in 2003. I had the good fortune to be taken on by CMRG a year later while continuing graduate school at UCSD, and would like to acknowledge the people who helped me get from inexperienced experimentalist to mouse surgeon and PhD scientist.

First I would like to thank my advisor, Andrew McCulloch, for his advice and input on all of my projects, poster presentations, talks, abstracts, and papers, as well as financial support. Whenever I had questions or problems, I always knew I would receive valuable and insightful feedback. Jeff Omens, co-chair of my committee, has also been instrumental in helping me set up data acquisition equipment and giving me advice on how to make my experimental goals more reasonable. I would like to thank Robert Sah, who advised me as an undergraduate research assistant, Robert Ross, and Francisco Villarreal for providing important perspectives as my dissertation projects evolved.

I would also like to thank Patrick Campbell, without whom this dissertation would not be possible. Patrick was a postdoctoral researcher at CMRG when I joined

the lab, and he taught me everything I know about mouse surgery. His work and guidance have contributed immeasurably to the projects presented here. Alexander Zambon is another scientist with a key role in this work. I have been quite fortunate to collaborate with him on the analysis of microarray data.

There are two longtime members of our group that I would especially like to acknowledge. Eleanore Hewitt has been the lab manager at CMRG since before I joined the group, and her help was instrumental in getting me started on my first project. Until a few years ago, Zhuangjie Li was the experimental guru of the lab, and he helped me more times than I can count with mice and equipment, always with a beaming smile and great senses of mischief and humor.

The student members of CMRG have all helped me in one way or another, whether it was giving me advice on a technique I was unfamiliar with, commiserating when our experiments failed, or celebrating together when we published a paper. In particular, Jody Martin helped me with immunofluorescent staining, Adam Wright has an uncanny ability to find just about anything in the lab, and Anna Jokiel taught me how to isolate RNA and perform PCR. I would also like to acknowledge several undergraduate students, now graduated or will be soon, who worked with me and whose assistance saved me many hours of work: Angie Li, James Kwok, Saleh Amiriazzi, Jun Shin, and Victor Chiu.

Finally, I would like to thank my family and friends for their love and support during the nearly six years I have been in graduate school. My parents, for always believing in me and being there for me, no matter what. My masters swimming and

later my UCSD Triathlon teammates, for providing me with a fun and competitive environment outside the lab. And most of all during the past year, Robert, whom I feel lucky to have met.

Chapter 2, in full, is a reprint of the material as it appears in: Campbell PH, Hunt DL, Jones Y, Harwood F, Omens JH, McCulloch AD, *Molecular and Cellular Biomechanics* 5(1):27-35, 2008; copyright Tech Science Press. Used with permission. The dissertation author was one of two primary investigators and authors of this paper.

Chapter 3, in part, will be submitted to the Journal of Molecular and Cellular Cardiology, with authors Hunt DL, Campbell PH, Zambon AC, Vranizan K, Omens JH, McCulloch AD. The dissertation author is the primary investigator and author of this material.

VITA

2009	PhD	Bioengineering	University of California, San Diego
2005	MS	Bioengineering	University of California, San Diego
2003	BS	Bioengineering	University of California, San Diego

HONORS AND AWARDS

- Jacobs School of Engineering Research Expo poster competition semifinalist, 2008
- National Science Foundation Graduate Research Fellowship Program Honorable Mention, 2005
- Graduated *magna cum laude*, 2003
- Outstanding Undergraduate Research Award, 2003
- Member, Tau Beta Pi Engineering Honor Society, 2001-2003
- Regents Scholarship, 1999-2003

PUBLICATIONS

Hunt DL, Campbell PH, Zambon AC, Vranizan K, Omens JH, McCulloch AD. Early Post-Myocardial Infarction Survival in Murphy Roths Large Mice is Mediated by Attenuated Apoptosis and Inflammation but Depends on Genetic Background (in preparation)

Jacot JG, Martin JC, **Hunt DL**. Mechanobiology of Cardiac Development. *Journal of Biomechanics* (2009, in review)

†Campbell PH, †**Hunt DL**, Jones Y, Harwood F, Amiel D, Omens JH, McCulloch AD. Effects of Biglycan Deficiency on Myocardial Infarct Structure and Mechanics. *Molecular and Cellular Biomechanics* (2008) 5(1):27-35 († co-first authors)

ABSTRACT OF THE DISSERTATION

MECHANISMS OF POST-MYOCARDIAL INFARCTION HEALING: FROM ACUTE SURVIVAL TO CHRONIC REMODELING

by

Darlene L. Hunt

Doctor of Philosophy in Bioengineering
University of California, San Diego, 2009

Professor Andrew D. McCulloch, Chair
Professor Jeffrey H. Omens, Co-Chair

Acute survival and chronic healing after myocardial infarction (MI) depend on a myriad of processes that begin within hours of the injury and can continue in the form of remodeling even years thereafter. The myocardium has very little self-renewal capability, and tissue lost to MI is replaced with a collagenous scar. There are currently no clinical therapies that directly target myocardial healing, due in part to the pleiotropic effects and redundancy of signaling factors released after injury. In addition,

some processes such as the inflammatory response are required for acute healing to proceed, but can also precipitate chronic deleterious remodeling and heart failure. A better understanding of the contributors to myocardial healing in both the acute and chronic phases is crucial in the search for clinical therapies that will improve the heart's response to MI injury.

In this work, we investigated the mechanisms of post-MI healing by studying two murine models of altered myocardial wound repair. We first studied infarct scar formation in mice lacking a proteoglycan with a role in collagen fibril assembly, and found that this deficiency altered infarct scar structure and mechanical properties compared to controls. Next, we investigated acute and chronic healing in a strain capable of myocardial regeneration after cryoprobe injury. Our results showed that this strain survives the acute phase and heals in the chronic phase post-MI better than a control strain, and that these differences could be attributed to reduced acute apoptosis and inflammation. The results presented here provide new insight into the mechanisms of post-MI survival and healing, and will be useful for future studies designed to improve mammalian cardiac repair.

1 Introduction

Heart disease is the leading cause of death in the United States [1], often a debilitating long-term result of myocardial infarction (MI). Coronary artery blockage, and the subsequent death of cardiac myocytes cut off from their blood supply, is a major cause of MI events. Only a small fraction of myocytes can divide [2,3], and healing consists largely of replacing necrotic cells with a collagenous scar [4,5]. Early complications can include pump failure and ventricular rupture, the latter accounting for up to 10% of acute mortality [6]. Forced to compensate for the loss of contractile tissue, the remaining myocardium experiences increased mechanical load, inducing global hypertrophy and dilation of the left ventricular (LV) cavity [4,7]. Although this remodeling process is initially successful in preserving some degree of cardiac function, the additional load imposed by LV enlargement can lead to further dilation [7] and a poor prognosis such as heart failure [4,5]. Because of its impact on public health, post-MI healing has been studied for several decades. This research has painted an increasingly complex picture of post-MI healing as a process that depends on a delicate balance

between myriad signals in the ischemic milieu. Here we review the time course of post-MI healing, with emphasis on events influencing the acute survival of the host and the formation of the collagenous infarct scar. Animal models with heightened and dysregulated healing processes will also be discussed.

1.1 Phases of Post-MI Healing

Healing after MI can be thought of as occurring in several overlapping phases, divided according to the timing and nature of the major processes involved [8,9], similar to classical wound healing [10-12]. The acute phase begins immediately after the cessation of blood flow to the region downstream of the blockage, and is characterized by cellular responses including myocyte necrosis, apoptosis, and robust inflammation, as well as thinning and expansion of the infarct. As part of the inflammatory response, cytokines and chemokines recruit neutrophils and macrophages to clear the infarct area of necrotic myocytes and extracellular matrix (ECM) debris. In experimental rodents, the acute phase lasts for roughly 4-7 days. Next, the injured heart enters the granulation and early remodeling phase, where new fibrous tissue begins to form after repression of inflammation. After approximately 21 days, mature collagen has been deposited and organized into a scar, but the late remodeling phase continues for weeks to months with a progressive decline in LV function if the infarct is large.

1.1.1 The Acute Phase

1.1.1.1 The Inflammatory Response

The complex post-MI healing response begins within hours of the ischemic insult [10,13-16]. One of the earliest events, between several hours to 1 day post-MI, is the release of pro-inflammatory cytokines and chemokines. Myocyte necrosis and the subsequent release of cellular contents triggers the complement cascade, activates pathways dependent on nuclear factor (NF)-κB and toll-like receptor (TLR), and generates reactive oxygen species, all of which contribute to inducing an inflammatory response [9]. Cytokines and chemokines exert a variety of effects on the myocardium in addition to attracting leukocytes to the infarct region (reviewed in Frangogiannis [9] and Nian et al. [10]). These effects can be beneficial and promote myocyte survival and wound healing [17], but also trigger apoptosis [18] and the recruitment of additional inflammatory mediators [19]. Robust inflammation induces matrix metalloproteinase (MMP) activity that in turn can lead to acute ventricular rupture [6,8,20,21], while chronic inflammation is associated with severe LV remodeling [21,22] and heart failure [22].

The post-MI inflammatory response is global, affecting the infarct region and its border, but also the remaining perfused area of the LV. In the first hours to 1 day post-MI in rodents, messenger RNA (mRNA) expression of cytokines, including tissue necrosis factor alpha (TNF-α), interleukin 1 beta (IL-1β), and interleukin 6 (IL-6), is upregulated up to 50-fold in the infarct region and 15-fold in the uninjured region of the LV [13,19]. Chemokines such as macrophage inflammatory protein (MIP)-1α, MIP-1β, and monocyte chemoattractant protein (MCP)-1 also appear to be markedly induced.

Increased expression of these factors has direct effects on cardiac myocytes and other cell types.

Inflammatory cytokines have been shown to influence cardiac myocyte survival in post-MI hearts, providing signals that promote or inhibit apoptosis. It appears that even individual cytokines are capable of providing both survival and death signals, and the balance between them determines the cell's fate. TNF receptor (TNFR1/TNFR2) knockout mice had larger infarct sizes and increased myocyte apoptosis compared to wildtype controls, suggesting a cytoprotective role for TNF-α in post-MI healing [17]. In contrast, TNF-α knockout mice had decreased myocyte apoptosis in the non-infarct region of post-MI hearts, as well as reduced LV dysfunction and a lower rate of LV rupture [21]. The effects of IL-6 and IL-1β on myocyte survival have been less well studied. Signal transduction upon binding of IL-6 to its receptor activates pathways including phosphatidylinositol-3 kinase [23], which provides cytoprotective signals. Mice with a targeted deletion of IL-6 were recently shown to have impaired cardiac function, increased interstitial fibrosis, and severe ventricular dilation [24]. However, an earlier study using mice lacking IL-6 did not find differences in infarct scar sizes or changes in cardiac function compared to wildtype controls after permanent coronary artery ligation [25], so the role of IL-6 with respect to cardiac myocyte survival remains unclear. Another cytokine which may influence myocyte survival after MI is erythropoietin (EPO). Mice injected with recombinant human EPO at the time of coronary artery ligation had a 50% reduction in apoptosis after 24 hours and significantly decreased infarct scar sizes 8 weeks later [26].

In contrast to the cytokines' direct action on cardiac myocytes, chemokines attract leukocytes to the infarct region. The CXC subfamily of chemokines contains neutrophil chemoattractants, while the CC subfamily recruits mononuclear cells [9]. Easily visible using routine hematoxylin and eosin (H&E) staining, neutrophils infiltrate the infarct border in great numbers, peaking approximately 2 days post-MI in the mouse [12]. Excessive neutrophil accumulation has been observed in the vicinity of ventricular ruptures compared to non-ruptured infarcts [27], suggesting a possible deleterious effect of neutrophils on myocardial injury. In fact, neutrophils are believed to be a major source of MMPs that have critical roles in causing ventricular rupture [28-30]. Macrophage infiltration peaks approximately 4 days post-MI in the mouse [12]. These cells are responsible for the phagocytosis of cell debris [16], and are also believed to be the source of some MMPs [30].

1.1.1.2 The Matrix Metalloproteinases

MMPs (reviewed by Spinale [31]) are responsible for degrading the proteins of the ECM left behind by necrotic myocytes, a process that must occur before the fragments can be accessed and phagocytosed by macrophages during healing. Members of the tissue inhibitor of metalloproteinase (TIMP) family are endogenous inhibitors of the MMPs [31], and the balance between MMP activity and TIMP expression determines the amount of ECM degradation. It has become well established that the MMPs and TIMPs play critical roles in cardiac pathology [6,8,28,29,32-40], with TIMP-1 and the gelatinases MMP-2 and MMP-9 being the most prominent in the setting of acute MI.

The gelatinases, MMP-2 (gelatinase A) and MMP-9 (gelatinase B) degrade denatured fibrillar collagens which have been cleaved at specific sites [33], as well as basement membrane components and other collagen types [31]. MMP proteins are expressed in pro-enzyme form, requiring cleavage by serine proteases to become active [30]. One of these serine proteases is plasmin, which has its own activators (urokinase and tissue-type plasminogen activator, uPA and tPA) and inhibitor (plasminogen activator inhibitor 1, PAI-1) that compose the plasminogen system [41]. After Heymans et al. [20] reported that MMP-2 or MMP-9 gene deletion protected against ventricular rupture, as did gene transfer of TIMP-1, many investigators began to characterize the time course of MMP and TIMP expression in the acute phase of MI. Ventricular rupture is a consequence of excessive infarct expansion [4], first described by Hutchins and Bulkley as thinning and elongation of the infarct that could not be explained by additional myocyte necrosis [42]. Histological examination revealed that myocyte bundles slipping relative to each other are responsible for the phenomenon [43]. Infarct expansion begins within 24 hours [43] and continues through the acute phase before extensive collagen deposition has occurred [4], a period when the ventricular wall is particularly vulnerable to mechanical deformation [44].

In the mouse, MMP-9 activity has been observed within 24 hours of the onset of ischemia, primarily in neutrophils [8,28,29], and continues to increase through day 3 post-MI [21]. MMP-9 activity begins to decline after this point, while MMP-2 activity begins to rise on day 4, peaks by day 7, and remains elevated for at least 2-4 weeks [8,29]. The sources of MMP-2 appear to be macrophages, fibroblasts, and myocytes [8,30,35]. Elevated

MMP activity is also present after MI in humans [6,36]. Perhaps not surprisingly, the time course of MMP activation correlates with inflammatory cell infiltration and the risk of ventricular rupture in mice, which is greatest between 3 and 5 days post-MI [8]. Genetic deletion of both MMP-2 [35,39,40] and MMP-9 [20] has been shown to protect against rupture. In humans, ruptured infarcts exhibit increased MMP-9 activity compared to infarcts that do not rupture [6].

Early increases in TIMP-1 mRNA expression have been reported, with expression rising by 3 days post-MI [45,46] and peaking by day 7 [46]. However, TIMP-1 protein is not significantly expressed until 2 weeks post-MI, indicating the presence of post-translational regulation [46]. Taken together, these studies suggest that excessive ECM degradation, mediated by MMPs released from infiltrating neutrophils and macrophages with little inhibition from TIMPs, occurs in the acute phase of post-MI healing and increases the risk of ventricular rupture.

1.1.1.3 Apoptosis

Cell death is clearly a prominent consequence of MI. Many myocytes, lacking a sufficient oxygen supply, die by necrosis and elicit an inflammatory response [9]. However, apoptosis is also an important feature of acute MI observed both experimentally and in humans (reviewed in Takemura and Fujiwara [47]), and occurs within hours of the ischemic insult [48,49]. As mentioned above, cell survival or death depends on the balance between multiple competing signals. One of the best-studied pathways leading to apoptosis is the death receptor pathway [50], which includes TNF signaling. The death receptor pathway involves the activation of Fas by binding of its

ligand (Fas ligand), which has been implicated in cell death after MI [51,52]. However, Fas activation has also been linked to induction of a transcription factor associated with hypertrophy [53]. Apoptosis can also be initiated in a mitochondrial-dependent manner. Regardless of the mechanism of activation, whether the apoptotic cascade continues or is inhibited may be subject to regulation by the Bcl-2 family of proteins, growth factors such as IGF-1, heat shock proteins, calcium-related effectors, and antioxidants (reviewed in Gill et al. [50]).

Various researchers have studied apoptosis in the setting of MI. Bialik and colleagues [48] showed that in the mouse, apoptosis is evident beginning about 4 hours after permanent coronary ligation and remains prominent through 2 days post-MI, declining thereafter. Terminal deoxynucleotidyl-transferase-mediated dUTP nick end labeling (TUNEL)-positive cells, those likely to be undergoing apoptosis due to the presence of DNA strand breaks, were found only in the hypoxic region. After 18 hours, about 9% of all nuclei counted in apical, midventricular, and basal sections (including both hypoxic and perfused regions) were TUNEL-positive. Other groups have reported the percentage of TUNEL-positive cells in the infarct region 24 hours after permanent occlusion: in mice, up to 55% [54], and in rats, up to 36% [26]. After ischemia/reperfusion, apoptosis is even more prominent than necrosis [55] and also occurs in the region surrounding the infarct [56]. Reductions in apoptosis early after MI have been shown to improve cardiac function and reduce adverse remodeling [26,57], so targeting apoptosis is becoming a therapeutic goal [50].

1.1.1.4 Limiting Myocardial Damage by Attenuating the Inflammatory Response, MMP Activity, or Apoptosis in Animals and Humans

Because of the heart's limited self-renewal capability, most myocytes lost to necrosis or apoptosis are replaced by non-contractile scar tissue that continues to remodel well past the time of initial injury. Viewed in this light, therapies administered in the early phase post-MI to limit myocardial damage may be the most promising strategies to improve patient outcome after MI. However, due to the pleiotropic effects and overlapping events of the major acute healing processes discussed above, care must be taken when attempting to alter them.

Inhibition of the inflammatory response has had considerable success in animal models [54,58-60] (and reviewed by Frangogiannis [9]). Many of these approaches directly target neutrophils (reviewed by Vinten-Johansen [61]). Depletion of neutrophils by specific filters or antibodies inhibiting adhesion has been shown to reduce infarct size of up to 50%. Of particular interest, a number of pharmacological anti-inflammatory agents have been used to limit neutrophil activation as well as neutrophil-mediated injury. In the 1980s, the non-steroidal anti-inflammatory drugs (NSAIDs) ibuprofen and cyclo-oxygenase inhibitors were successfully tested in animal models. However, clinical testing of some NSAIDs was quite the opposite. Patients receiving ibuprofen had greater infarct thinning and lengthening than patients not receiving anti-inflammatory therapy [62], and some patients receiving high doses of methylprednisolone suffered ventricular aneurysm and rupture [61,63]. These results indicate that even though post-MI inflammation is associated with deleterious effects, it remains an important

process necessary for proper infarct healing. More recently, the clinical trials LIMIT-MI [64] and HALT-MI [65] failed to show any difference in infarct size after treatment with antibodies intended to limit neutrophil adhesion, which had been successful in animal experiments. This suggests that important components of the inflammatory response in animals may not necessarily be relevant in humans.

Much effort has also been put into the limitation of plasminogen and MMP activity in the acute phase post-MI, whether by gene deletion or pharmacological inhibition, to reduce ventricular rupture and adverse remodeling [20,32,35,37-40,66]. One of the earliest studies of plasminogen activator and MMP gene deletion in mice reported complete protection against ventricular rupture in $uPA^{-/-}$ mice, and partial protection in MMP-$9^{-/-}$ mice [20]. Additional studies using MMP-2 gene deletion [39,40] and pharmacological inhibition [40] have shown that lack of MMP-2 activity may also protect against rupture in mice. However, lack of rupture is not always associated with a desirable outcome. Wound healing was severely impaired in $uPA^{-/-}$ mice; inflammatory cell infiltration was reduced by nearly 50%, necrotic myocytes had not been phagocytosed even 5 weeks after MI, and there was very little new collagen deposition [20]. Another study showed that deletion of the plasminogen gene also prevented proper wound healing after MI [66]. These results highlight the need for at least some plasminogen-MMP system activity to successfully repair the injured heart. In a similar vein, selective MMP inhibition using pharmagological agents has been attempted in non-rodent animals [67,68] and humans [38]. Administered 1 day post-MI in rabbits, selective MMP inhibition reduced ventricular wall thinning and dilation 4 weeks later [67]. In pigs,

the inhibitor was administered either 3 days before or 3 days after MI, and the pre-MI administration was associated with impaired wound healing compared to the post-MI administration [68]. These studies show that selective MMP inhibition may have therapeutic potential, but that the timing of inhibitor administration should be carefully considered. However, a study of selective inhibition of MMPs in humans did not find any significant differences in clinically relevant endpoints such as left ventricular volume and ejection fraction [38]. In experimental animals, endogenously inhibiting the plasminogen-MMP system using PAI-1 or TIMP-1 has been shown to protect against rupture [20]. This therapeutic approach does not appear to be proceeding in human trials.

Reduction of apoptotic cell death in the acute phase post-MI may be another therapeutic avenue to reduce adverse ventricular remodeling due to loss of myocytes. Heat shock proteins (Hsps) and their cofactors, which play numerous roles in protein folding and trafficking, have been shown to inhibit both apoptotic and necrotic pathways [69]. Overexpression of Hsp70 reduced infarct size and improved cardiac function after ischemia/reperfusion (I/R) [70]. Lack of CHIP, a cochaperone that interacts with Hsp70, resulted in decreased survival, larger infarct size, more apoptosis, and poorer functional outcome after I/R [71]. CHIP interacts with Hsp70 to re-fold proteins damaged by stress, such as ischemia, and also acts as a ubiquitin ligase [71]. Proteins too damaged to be re-folded are then destroyed via proteasome-dependent pathways. Through these activities, cochaperones and heat shock proteins may assist in increasing survival and reducing infarct size by limiting apoptosis. Other studies designed to affect myocyte survival post-MI showed that administration of recombinant human

erythropoietin (rhEPO) markedly attenuated apoptosis in models of permanent coronary occlusion [26] and I/R [72], in addition to reducing infarct size and improving LV function. Antioxidants, IGF-1 and the Bcl-2 family of proteins may also affect apoptotic pathways in the heart (reviewed in Gill et al. [50]). In humans, an increased level of serum EPO has been associated with smaller infarct size as measured by serum creatine kinase level [73]. Safety and feasibility pilot studies of EPO administration have been conducted in patients with MI [74] and non-ST segment elevation myocardial injury [75], and four larger phase II randomized, controlled trials are underway [76].

From the above, it is clear that the acute phase of post-MI healing can be altered to improve survival and healing in experimental animals. However, since processes such as the inflammatory response and ECM degradation mediated by the plasminogen-MMP system are required for proper healing, it is important to avoid abolishing them completely. The timing of interventions designed to interfere with acute healing processes is also critical, due to the sharp increase in apoptosis just hours to one day post-MI and the different waves of inflammatory infiltration and MMP activity. Therapies targeting the acute healing phase hold great promise, but much more research must be done before clinical benefits can emerge.

1.1.2 The Granulation and Early Remodeling Phase

Beginning about 4-5 days post-MI in mice, granulation tissue rich in ECM proteins begins to form as myofibroblasts and endothelial cells proliferate, and macrophages continue to phagocytose the remaining necrotic myocardium [77]. As

healing continues, myofibroblasts deposit collagen that will be organized into the infarct scar, and the granulation tissue begins to be reabsorbed [30]. By about 21 days post-MI, granulation tissue absorption is complete and a collagenous scar remains.

In order for healing to proceed optimally, continuous leukocyte infiltration and cytokine/chemokine expression must be suppressed to avoid further injury [9]. Several processes may be important in the transition from inflammation to fibrous tissue deposition. The anti-inflammatory cytokine IL-10 inhibits the production of several pro-inflammatory cytokines [78] and may also stimulate TIMP-1 synthesis [79], promoting decreased ECM degradation. Phagocytosis of apoptotic neutrophils by macrophages leads to the release of tissue growth factor (TGF)-β, an important pro-fibrotic cytokine which also aids in inflammatory resolution [80].

TGF-β signaling may be critical in the setting of early post-MI remodeling. Inhibition of its signaling activity by adenoviral transfection of TGF-β receptor type II (TBR-II) exacerbated the decline in LV function 9 hours after MI in mice, accompanied by decreased survival, increased neutrophil infiltration, and enhanced cytokine expression compared to animals with MI and no TBR-II treatment [81]. However, after 28 days chronic LV dilation was attenuated and ventricular function was improved. These results support the idea that TGF-β signaling is beneficial in early post-MI remodeling as a suppressor of the inflammatory response. Additionally, its signaling activity may promote the deposition of the granulation tissue itself by stimulating fibroblasts to deposit ECM proteins such as collagens, proteoglycans, fibronectin [82], osteopontin, and

thrombospondins [83], as well as by inducing the expression of proteinase inhibitors such as TIMP-1 and PAI-1 [82].

MMPs remain active during the early remodeling phase. After peaking in the acute phase, MMP-9 and MMP-2 activity both decrease but are still significantly elevated through 2 weeks post-MI [8,20,39,46]. MMP-8, which degrades fibrillar collagen, is significantly expressed after 2 weeks and remains elevated thereafter [46]. Several other MMPs are also expressed [30]. A complement of active MMPs capable of degrading collagens and the granulation tissue in the healing infarct balances the expression of TIMPs and collagen deposition by myofibroblasts, enabling a dynamic and continuous remodeling process.

1.1.3 The Late Remodeling Phase

By 21 days after MI, the granulation tissue has been resorbed, many macrophages and myofibroblasts have undergone apoptosis [84], and the healed infarct becomes a collagenous scar. However, the heart is not in a static state. Under the influence of continued inflammation, expression of MMPs [85], apoptosis [50], and mechanical factors [4,7], ventricular remodeling continues for months to years after the initial injury in both the infarct and non-infarct regions and often leads to heart failure.

The processes of inflammation, MMP activity, apoptosis, and collagen deposition are closely intertwined. In the early stages of heart failure, inflammation stimulates increased MMP activity analogous to that observed after MI, but prolonged exposure appears to induce TIMP and TGF-β expression, shifting the balance toward

collagen deposition [86]. Cytokines such as TNF-α may stimulate apoptosis after MI [21], and cell death has been observed in heart failure [87,88].

Even after the resolution of the inflammatory response in the early remodeling phase, hearts with large infarcts or other stressors are vulnerable to a second wave of inflammation in the non-infarct region that precipitates remodeling. Cytokine gene expression is significantly elevated in the non-infarct region compared to the infarct region 20 weeks post-MI in rats [89]. Further, cytokine expression levels are positively correlated to LV end-diastolic diameter, and IL-1β expression is correlated with interstitial fibrosis in the non-infarct region. In addition to the influence of mechanical factors, studies using transgenic mice overexpressing TNF-α have shown that cytokine is capable of stimulating myocyte hypertrophy [90,91]. In these models, apoptosis was increased [90], as was collagen deposition and TGF-β expression [91].

The infarct scar itself is a living tissue that can dynamically remodel well after the initial injury [92]. Myofibroblasts are thought to be the primary source of collagen deposited in the infarct region, as well as TGF-β during the late remodeling phase, while cardiac fibroblasts are thought to be responsible for collagen deposition in the non-infarct region [92]. Myofibroblasts are phenotypically modified cardiac fibroblasts, stimulated to transform by TGF-β [93], TNF-α, and IL-1β [86], that express α-smooth muscle actin and mediate contraction of the scar into a more compact structure as it matures. The immature scar is composed of mostly type III collagen, which is more distensible than the type I collagen deposited at later stages [85]. After about 13-15 weeks, the type I/type III collagen ratio has increased and cross-links have formed, further

strengthening the scar [85]. Some collagen turnover still occurs after this time; myofibroblasts have been detected up to 17 years after MI in humans [94].

The presence of a non-contractile, stiff scar segment in the LV myocardium increases the stress experienced by the healthy tissue, which dilates to preserve stroke volume, further increasing wall stress [95]. The severity of dilation depends on the size of the initial infarct [96], and is due to a rearrangement of myofibrils rather than stretching of sarcomeres [4]. In response to the loss of contractile mass, the remaining healthy myocytes undergo hypertrophy [97]. However, this compensatory process often fails with large infarcts since too many myocytes have been lost [97], and could also be related to energy wasted stretching the scar during systole [95]. These hearts are at greatest risk of pump failure. In patients, LV dilation is associated with increased mortality [4,22].

1.2 Dysregulated Collagen Assembly and its Effect on Wound Healing

As discussed above, collagen deposition is an integral part of scar formation after MI. Beside the contribution of cytokines, MMPs, and TIMPs to overall collagen content, the assembly of the collagen molecule is itself regulated. Here we briefly discuss the regulation of collagen assembly, or fibrillogenesis, and how defects in this regulation affect wound healing in the heart and other tissues.

The collagen molecule is translated as three separate peptide α chains that assemble into a superhelix structure [98]. These structures aggregate to form collagen microfibrils, and further to become fibrils. Many different collagen types are found in

various tissues, but the fibrillar type I and type III collagens constitute the bulk of the cardiac ECM, with type I accounting for about 85% and type III for about 11% of the collagen content [85].

Small leucine-rich proteoglycans (SLRPs) have been shown to regulate collagen fibril assembly in vivo [29,99-101], and all tissues contain at least one member of this family [102]. Decorin and biglycan, the best-studied of these ECM macromolecules, have been shown to bind type I collagen [103] and likely affect lateral aggregation of collagen fibrils [104], thereby regulating their diameter. The effects of genetic SLRP deletion have been investigated in several studies. Biglycan/fibromodulin double knockout mice had mechanically compromised patellar tendons, developed tendon ossification, and had severe osteoarthritis [99]. In the same study, electron microscopy showed that biglycan-null and double-knockout quadriceps tendons had smaller collagen fibril diameters. In the endometrium of the uterus, the loss of thin collagen fibers and an increase in thick fibers has been correlated with the appearance of biglycan and the loss of two other SLRPs, decorin and lumican [101]. Differing fibril diameters have also been observed in the proximal predentin of biglycan-null mice [100], and in decorin-null hearts [29]. Biglycan-null mice have an osteoporosis-like phenotype [49,105] and the males are susceptible to aortic rupture [106], and decorin-null mice have fragile skin with reduced tensile strength [107].

Deficiency in SLRPs can also lead to cardiac effects that have only recently been investigated [29,108]. Decorin-null mice subjected to permanent coronary occlusion had a wider distribution of collagen fibril diameters present in the infarct scar compared

to wildtype mice, and this was accompanied by significantly larger infarct scar size, LV dilation, and depressed systolic function [29]. In biglycan-null mice, coronary occlusion did not lead to larger infarct scars, but the scars were stiffer and had a tighter distribution of collagen fibril diameters than the wildtype [108]. This study will be discussed in detail in Chapter 2.

1.3 Heightened Wound Healing and Regeneration

The adult mammalian heart has very little capacity for self-renewal [3], in contrast to organisms such as the urodele newt [109] and zebrafish [110]. However, fetal mouse hearts in culture are capable of regenerating linear wounds up to about embryonic day 14 [111], suggesting that the ability to regenerate exists but is suppressed in adult tissues. The discovery that the adult mammalian heart may in fact have a resident progenitor cell population [112-117] has spurred efforts to coax it into activity after injury [112,118-120]. Here we briefly discuss regeneration and efforts to apply it to mammalian tissues, and introduce a mouse strain that may lend insight into the possibility of mammalian regeneration.

Regenerative wound healing is characterized by a proliferative response [109,110] rather than inflammation and scarring as in most adult tissues [121], resulting in a recapitulation of normal tissue architecture. Stem cells have been a focus of recent research because of their ability to proliferate and differentiate into multiple lineages, raising the possibility of exploiting those properties to regenerate adult tissues. Mounting evidence suggests that mammals, including humans, have a population of

endogenous cardiac progenitor cells (CPCs) that can differentiate into myocytes [112-117], smooth muscle cells, and endothelial cells [115,119]. Though there are different populations of cells in the myocardium that express stem cell markers (c-kit, Sca-1, MDR-1) and are not blood-derived (lineage negative, Lin^-) [112,119], the most recent research has focused on the $Lin^-c\text{-}kit^+$ population [115,118]. Studies have shown that CPCs are responsive to stimulation by hepatocyte growth factor (HGF) and insulin-like growth factor 1 (IGF-1), which promotes the survival, proliferation, and migration of the CPCs [112,120]. Intramyocardial injection of HGF and IGF-1 in mice [120] and dogs [112] has been shown to induce CPCs to reconstitute myocytes and coronary vessels following MI, reducing the scarred area. In mice, this treatment also increased survival [120].

In the last 10 years, a strain of mice with the intriguing ability to regenerate different tissue types has received attention. An accidental discovery first revealed that the lymphoproliferative (lpr) Murphy Roths Large-Fas^{lpr} (MRL- Fas^{lpr}) mouse and its control, the MRL/MpJ (MRL), are capable of regenerating through-and-through ear punches used for colony marking [122]. Healing was accompanied by normal tissue growth, including angiogenesis and chondrogenesis, and perhaps the most striking, a blastema-like structure reminiscent of amphibian limb regeneration. Subsequently, Leferovich and colleagues reported that MRL mice are capable of regenerating right ventricular myocardium after cryoprobe injury [123], and found that up to 20% of myocytes in the wound region were positive for 5-bromo-2'deoxyuridine (BrdU), a marker of cell division, compared to a maximum of 4% in the C57BL/6J controls. The source of the BrdU-positive cells is unknown, but could potentially include a population

of CPCs. Replacing the bone marrow of lethally irradiated female MRL mice with bone marrow from male MRL mice yielded no double labeling for BrdU and Y chromosome after cryoinjury, suggesting that the cells contributing to regeneration are not hematopoietic [124]. Several groups have studied the more clinically relevant model of coronary artery ligation [125-130]. Results indicated that the MRL heart heals with a scar after MI, but there was evidence for increased survival, stabilization of cardiac function, and BrdU-positive myocytes [130]. The response of the MRL mouse to coronary artery ligation will be discussed in detail in Chapter 3.

1.4 Conclusions

A large body of work has advanced understanding of the biological processes involved in post-MI healing. In the acute phase, cell death by necrosis and apoptosis is prominent, and these are accompanied by a robust inflammatory response and MMP activity. Resolution of the inflammatory response and collagen deposition begin in the early remodeling phase. Collagen deposition and degradation continues through the later remodeling phase, when the granulation tissue has been replaced with a scar.

The acute phase of post-MI healing has been studied extensively to determine the time course of events, and the importance of major biological processes such as inflammatory infiltration, apoptosis, and MMP activity. Each of these is induced soon after ischemic injury. Studies have shown that interventions attempting to attenuate or eliminate the activity of inflammation and MMPs must carefully consider the timing

and breadth of inhibition to avoid impairing wound healing. Experiments designed to attenuate apoptosis have been promising and are progressing in clinical trials.

The processes mentioned above can also be important in the late remodeling phase if the infarct is large, and acute interventions that reduce the severity of the initial response to injury may also attenuate ventricular remodeling. The regulation of collagen fibrillogenesis may contribute to the severity of remodeling by altering the scar microstructure, rendering it more susceptible to distension. The presence of proteoglycans may be critical for proper scar organization.

The MRL mouse may provide a new avenue to study post-MI healing in both the acute and chronic phases, by virtue of its unusually high acute survival rate and increased chronic BrdU incorporation. Investigating the mechanisms underlying its survival, which are likely to include alterations in one or more of the above biological processes, may lead to new insights into methods of improving early post-MI survival. Studying chronic healing in the MRL may contribute to our understanding of regeneration in mammalian tissues.

1.5 Scope of the Dissertation

The objective of this dissertation was to investigate the role of abnormal regulation of wound healing in post-myocardial infarction cardiac repair. Specifically, we studied the effect of deleting an ECM proteoglycan on chronic healing, and investigated the mechanisms that could be responsible for heightened acute survival and healing in a model of myocardial regeneration.

Chapter 2 describes the first characterization of the role of the proteoglycan biglycan in post-MI healing. This involved creating MI in biglycan-null mice, and studying the structural and mechanical properties of the infarct scar.

Chapter 3 describes the elucidation of the mechanisms that could be responsible for increased survival in the MRL mouse, and the characterization of its chronic healing capability. This involved comparing post-MI survival and healing in the MRL and two other strains of mice, including the major genetic background of the MRL. Hypotheses regarding increased survival mechanisms were generated using a microarray analysis, and confirmed with tissue-level assays. Chronic infarct scar size and cell proliferation were also compared.

Chapter 4 summarizes these studies and their contributions to our understanding of post-MI survival and remodeling, and provides a perspective on how their results could impact the design of therapies to improve cardiac healing.

2 Effects of Biglycan Deficiency on Myocardial Infarct Structure and Mechanics

2.1 Abstract

Biglycan, a small leucine-rich proteoglycan, has been shown to interact with extracellular matrix (ECM) collagen and may influence fibrillogenesis. We hypothesized that biglycan contributes to post-myocardial infarction (MI) scar development and that the absence of biglycan would result in altered scar structure and mechanics. Anterior MI was induced in biglycan hemizygous null and wild-type mice by permanent ligation of the left coronary artery. The initial extent of ischemic injury was similar in the two groups, as was the infarct size after 30 days, although there was some tendency toward reduced expansion in the biglycan-null. Electron microscopy revealed that collagen fibrils had a smaller average diameter and a narrower range in the biglycan-null scar, as well as appearing more densely packed. *In vivo* strain analysis

showed that biglycan-null scars were stiffer than the wild-type. Remote LV collagen concentration tended to be reduced in biglycan-null hearts, but the difference was not statistically significant. Null-expression of biglycan may alter collagen fibril ultrastructure, and thereby influence scar mechanics and remodeling.

2.2 Introduction

Under normal and pathological conditions, the structure and mechanics of the mammalian heart depend critically on the extracellular matrix (ECM). Collagen, a major component of the ECM, is organized in an intricate three-dimensional network surrounding and connecting the muscle fibers. This network facilitates the transmission of forces between fibers, and across the ventricle walls during the cardiac cycle [131,132]. In addition to its role as a force transmitter, the collagen ECM supplies the structural stability and elasticity necessary for proper pump function.

The death of myocytes during myocardial infarction (MI) induces major structural alterations collectively known as ventricular remodeling. During the acute phase after injury, necrotic tissue and its ECM are resorbed while a fibroproliferative response produces a scar rich in Type I collagen to preserve the tensile strength of the ventricle wall [5]. The extent of remodeling in the ischemic region depends on the balance between these two processes. Imperfect coordination can result in thinning and elongation of the infarct region before extensive collagen deposition has occurred [5]. The stiffness of the mature scar depends on collagen type, crosslinking, arrangement, and size and number of fibers [95,133]. Because it is thin and has a high local radius of

curvature, the stresses observed in the scar are considerably greater than those in the unaffected region of the ventricle [95]. Interestingly, in passively inflated hearts the scar was found to be anisotropic, resisting circumferential deformation more so than longitudinal or radial. Most large collagen fibers were aligned with the circumferential axis, suggesting that increased stiffness in the circumferential direction may help maintain proper ventricular mechanics [95]. Thus scar structure is organized to accommodate the stresses imposed during the cardiac cycle.

There is substantial evidence that the regulation of fiber assembly and organization of fibers in infarct scar tissue, as well as other collagenous tissues, depend in part on a group of ECM macromolecules known as proteoglycans [29,103,134,135]. One such macromolecule is the small leucine-rich proteoglycan (SLRP) biglycan. Biglycan is a widely expressed protein localized to the interstitium and cell surface [136]. Depending on the tissue type, the biglycan core has one or two chondroitin sulfate or dermatan sulfate groups at the amino terminus [137].

Little is known about biglycan's function and its role in collagen fibrillogenesis, especially in the heart. However, biglycan binds collagen type I and TGF-β1, an important factor in driving fibrillogenesis [103,138]. The physiological or pathophysiological roles of biglycan in the heart are largely unknown, though some evidence suggests a possible function in post-MI healing. Biglycan mRNA has been shown to increase in the rat heart 2 days post-MI, with a 13-fold peak by day 14, and to co-localize with collagen type I mRNA [139].

Our lab has previously studied the role of another SLRP, decorin, in post-MI healing. Infarct scars of transgenic mice lacking decorin were structurally dysregulated, and collagen fibrils had non-uniform diameter. This may have compromised the scar's ability to resist stress, and resulted in the observed infarct expansion. Increased left ventricular dilation also led to greater hypertrophy of the remote, uninjured region [29]. Since decorin has a similar structure to biglycan, even competing for binding sites on type I collagen [101], we hypothesized that similar structural dysregulation would occur in biglycan-null mice after experimental MI, and that the infarct scar mechanical properties would also be affected. In the present study, we induced MI in biglycan hemizygous-null mice and found altered collagen fibril structure in infarct scar tissue, and changes in scar mechanics compared with wild-type controls. There was evidence that lack of biglycan actually allows a denser scar with smaller, more uniform collagen fibrils that are more resistant to expansion.

2.3 Methods

2.3.1 Animals and Surgery

All animal studies and husbandry were conducted under approved University of California, San Diego Animal Subjects Protocols in AAALAC-approved facilities. Breeding pairs of female homozygous biglycan-deficient (*Bgn*$^{-/-}$, strain name: C3.129S4(B6)-Bgn $^{tm1Mfy/Tac}$) and male hemizygous biglycan-deficient (*Bgn*$^{-/0}$) mice were obtained from the Mutant Mouse Regional Resource Centers through Taconic Farms, Inc., and bred at our breeding facility. Since the biglycan gene is located on the

X chromosome, male biglycan-null mice are referred to as hemizygous. Male 12-18 week-old *Bgn*$^{-/0}$ mice were used for this study. Male age-matched C3H mice (*Bgn*$^{+/0}$), also obtained from Taconic, were used as controls. The C3H strain is the background of the biglycan-null, and the recommended control.

MI surgery was performed using a procedure similar to that described by Weis et al. [29]. Mice were anesthetized with the inhalant anesthetic isoflurane at 5.0% in 100% oxygen, and maintained at 2.0% delivered to the spontaneously breathing animal through a nose cone. The trachea was surgically exposed, the tongue was retracted, and intubation was performed with a 20-gauge angiocatheter. The animal was placed on a rodent ventilator (Harvard Apparatus, Model 687), and ventilated with 2% isoflurane in 95% oxygen at a flow rate of 1 L/min and a stroke volume of 0.5 ml at 85 breaths/min. A 1.5 cm vertical left parasternal skin incision exposed the underlying pectoralis muscles, which were then retracted. The heart was exposed by entering the chest cavity through the third intercostal space and retracting adjacent ribs. The left coronary artery was ligated with 7-0 silk suture approximately 2 mm below the edge of the left atrial appendage. Ischemia was verified visually by the appearance of paleness on the surface of the left ventricle distal to the ligation. The lungs were overinflated, and the chest cavity was closed by suturing the adjacent ribs together with 6-0 prolene. The chest and neck skin incisions were then closed with prolene suture. Animals received 0.1 mg/kg buprenorphine intraoperatively for analgesia. After removal from the ventilator, animals awakened on a water-circulating heating pad (K Module, American Pharmaseal) and

were placed in a clean, heated cage to recover. Surgery was performed with the aid of a stereomicroscope (Leica Microsystems MZ6).

2.3.2 Initial infarct size

A subset of animals (7 *Bgn*$^{+/0}$ and 9 *Bgn*$^{-/0}$) was studied one day after MI to determine the initial infarct size. Animals were anesthetized with isoflurane, the thoracic cavity was opened, and the hearts were arrested with an ice-cold, hyperkalemic Krebs-Henseleit buffer containing 2,3,5-Butanedione monoxime to delay the onset of contracture. The atria and right ventricle were removed, and the left ventricle (LV) was wrapped in plastic wrap, then placed in a -20˚ C freezer for 1 hour. The LV was then placed in a cutting fixture with slits spaced 1 mm apart, and sliced into 1-2 mm short axis sections. The slices were stained with triphenyl tetrazolium chloride (TTC), then squeezed between two Plexiglas plates with 1mm spacers. This apparatus was placed in a shallow tray of water and photographed with a digital camera (Nikon Coolpix 4500) mounted on a Leica MZ6 stereomicroscope [140,141]. Healthy tissue stains dark red, while unstained tissue marks the infarct area. Using ImageJ (NIH), total tissue area and infarct area were measured for both sides of each LV section and averaged. Infarct size was expressed as a percentage of infarct volume to total LV tissue volume.

2.3.3 Histology and light microscopy

A second group of 7 *Bgn*$^{+/0}$ and 8 *Bgn*$^{-/0}$ mice was studied 30 days after MI for measurement of infarct size. Animals were anesthetized with isoflurane, and the

thoracic cavity was opened to expose the heart. Hearts were removed and arrested with the same Krebs-Henseleit buffer, then rinsed and prepared for paraffin embedding. Short axis sections 10 μm thick were taken from apex to base and stained using picrosirius red as previously described [142]. A light microscope (Olympus BH-2) with a 2X objective was used in conjunction with a Spot-RT camera to obtain digital images. Infarct size was determined using a technique modified from Pfeffer *et al*. [5]. Image J measurements of eight to ten equally spaced sections were used to determine the infarct size, expressed as a percentage of infarct area to total LV tissue area.

2.3.4 Transmission electron microscopy

Infarct scar tissue from 2 animals of each genotype was isolated from the rest of the heart 30 days post-MI. The tissue was prepared as previously described [29], and imaged with Jeol-100CX microscopy to obtain cross-sectional and longitudinal views of collagen fibrils at 20,000 and 50,000× magnification. Cross-sectional diameter measurements were made with ImageJ.

2.3.5 Biochemistry

30 days post-MI, the remote LV was removed from 6 $Bgn^{+/0}$ and 4 $Bgn^{-/0}$ hearts. Collagen concentration, as measured by hydroxyproline content, was determined using the method of Woessner [143]. Pyridinoline content was quantified to measure nonreducible crosslinks, using a method modified [144] from Eyre et al. [145].

2.3.6 Pressure and strain measurements

Four animals of each genotype were anesthetized and intubated as described above, and the right carotid artery was isolated. A 1.4 french Mikro-Tip catheter (SPR-839, Millar instruments) was advanced down the right carotid artery to the aorta and then the LV. Continuous LV pressure was recorded at steady-state conditions, with the animal's body temperature closely monitored and maintained at 37˚C with a water-circulating heating pad (K Module, American Pharmaseal). The chest was then opened to expose the heart. Titanium dioxide markers were placed on the infarct scar and videotaped using a CCD camera (COHU Inc.). Temporal resolution was increased to 60 Hz by splitting the videotape frames into fields with Scion Image (Version Beta 4.0.2). To stabilize the heart for videotaping, cotton was used as an added support and the ventilator was briefly turned off. Three marks on the infarct scar were used to determine two-dimensional epicardial area strain throughout the cardiac cycle, defined as the product of the two principal stretch ratios. The field with minimum distance between the points was used as a reference. Frame markers recorded along with the LV pressure allowed the identification of a pressure for each recorded frame [146].

2.3.7 Statistics

All data were analyzed with one- or two-way ANOVA or Student's t tests, with Welch's correction if necessary, at a significance level of 0.05. Data are presented as mean ± SEM.

2.4 Results

2.4.1 Infarct size

As assessed by TTC staining, there was no significant difference in the initial infarct size distribution one day post-MI between genotypes ($Bgn^{+/0}$ 32.2 ± 4.7%, n=7 vs. $Bgn^{-/0}$ 35.1 ± 5.2%, n=9; P=0.6, Figure 2.1). Infarct sizes were also not significantly different after 30 days, as determined by histological analysis ($Bgn^{+/0}$ 43.1 ± 1.9%, n=7 vs. $Bgn^{-/0}$ 40.2 ± 2.8%, n=8; P=0.4, Figure 2.2). The change in infarct size from 1 to 30 days post-MI was twice as great in $Bgn^{+/0}$ hearts compared to $Bgn^{-/0}$ hearts, but since it was not possible to study the same animals at the two time points, this difference was not significant (P~0.5).

2.4.2 Infarct scar ultrastructure

The ultrastructure of $Bgn^{+/0}$ and $Bgn^{-/0}$ infarct scars was investigated using electron microscopy. A longitudinal view of collagen fibrils from each genotype is shown in Figure 2.3. No differences were observed in the longitudinal structure of the individual fibrils and the arrangement of fibrils forming the scar tissue. However, a cross-sectional view revealed that collagen fibril diameter was smaller in $Bgn^{-/0}$ scars (Figure 2.4B) than in $Bgn^{+/0}$ scars (Figure 2.4A). Measurement of a random sample of 100 fibrils from 2 animals of each genotype showed that both their diameter and cross-sectional area were significantly smaller in $Bgn^{-/0}$ than $Bgn^{+/0}$ scars (diameter: 37.7 ± 0.6 nm vs. 46.9 ± 0.8 nm, P<0.0001; area: 1138 ± 33 nm^2 vs. 1773 ± 55 nm^2, P<0.0001; Figure 2.4C, D). Interestingly, the variance in fibril diameter and cross-sectional area

was significantly smaller in *Bgn*$^{-/0}$ scars (P<0.005). Histograms showed that the two highest frequency bins (35 and 40 nm) comprised 68% of *Bgn*$^{-/0}$ fibril diameters (Figure 2.4F), while the two *Bgn*$^{+/0}$ high frequency bins (45 and 50 nm) included only 48% of fibrils (Figure 2.4E). From the representative images in Figure 2.4A and B, it appears that the fibrils are more closely packed in *Bgn*$^{-/0}$ than *Bgn*$^{+/0}$ scars, though this was not quantified.

2.4.3 LV collagen concentration

Collagen concentration was measured in both the infarct and non-infarct region of the LV in both genotypes (Figure 2.5), and crosslinking was quantified in the infarct region. The concentration is expressed as a percentage of total non-infarcted LV dry weight. Collagen concentration was not significantly different in the infarct region of *Bgn*$^{+/0}$ and *Bgn*$^{-/0}$ hearts (30.02 ± 1.95%, n=6 vs. 32.95 ± 3.00%, n=7, P=0.4; Figure 2.5A). There was a trend toward greater collagen concentration in the remote region of *Bgn*$^{+/0}$ hearts compared to the *Bgn*$^{-/0}$ hearts (1.80 ± 0.12%, n=6 vs. 1.47 ± 0.07%, n=4, P=0.07; Figure 2.5B). Collagen crosslinking, as determined by pyridinoline content, was not significantly different between genotypes (0.43 ± 0.15%, n=3 vs. 0.34 ± 0.7, n=7, P=0.6; data not shown).

2.4.4 Strain analysis

In vivo strain analysis was performed directly on the infarct scar 30 days post-MI in *Bgn*$^{+/0}$ and *Bgn*$^{-/0}$ mice. Averaged area strain for 4 animals of each genotype over

approximately 4 cardiac cycles is shown in Figure 2.6. ANOVA showed a significant difference between the curves; strain was significantly smaller in $Bgn^{-/0}$ than in $Bgn^{+/0}$ scars (P=0.005). Consistent with the collagen fibril diameter results presented above, the variability in strain was smaller in $Bgn^{-/0}$ scars than in $Bgn^{+/0}$ scars. Simultaneous conductance catheter pressure measurements were averaged in a similar manner and plotted against strain; Figure 2.7 depicts the pressure-strain curve for each genotype. Two-way ANOVA showed that $Bgn^{-/0}$ scars were significantly stiffer (P=0.01).

2.5 Discussion

This study investigated the role of the SLRP biglycan in post-myocardial infarction healing and remodeling. Collagen fibril diameter and cross-sectional area were significantly smaller in $Bgn^{-/0}$ infarct scars 30 days post-MI than in $Bgn^{+/0}$ scars. Fibrils were also more closely packed, which may have led to the significantly increased stiffness and reduced variability of $Bgn^{-/0}$ scars observed during *in-vivo* strain analysis. These scars expanded half as much as their $Bgn^{+/0}$counterparts. However, owing to the inherent variability of infarct size in coronary ligation studies, and since we did not have a means for longitudinal measurement of infarct size *in vivo* throughout the study period, the sample size was not large enough for this difference in post-infarct remodeling to achieve statistical significance. A trend toward reduced collagen concentration in the remote LV further supported this reduction in remodeling severity. Here we show for the first time that lack of biglycan induces ultrastructural changes in the mouse heart, and that these may lead to a stiffer scar that resists expansion more

effectively than the wild-type, thereby reducing the severity of remodeling in the chronic phase of MI.

Little research exists on the collagen ultrastructure of the biglycan-null mouse, but there are some similarities between the present study and previous reports [99,100]. Smaller collagen fibril diameters were observed in the proximal predentin of *Bgn*$^{-/0}$ mice compared to *Bgn*$^{+/0}$, while other regions had larger diameters [100]. Ameye and colleagues [99] reported that patellar tendons from biglycan/fibromodulin double-knockout mice had a significantly different range and distribution of collagen fibrils than wild-type, and that double-knockout fibrils were smaller. In the endometrium of the uterus, the loss of thin collagen fibers and an increase in thick fibers was correlated with the appearance of biglycan and the loss of two other SLRPs, decorin and lumican [101]. Finally, the reported range of collagen fibril diameters in the normal mammalian heart is 30-70 nm [147], consistent with the *Bgn*$^{+/0}$ infarct scars in the present study.

Our laboratory has examined another SLRP, decorin, and its role in post-MI healing. Decorin-null infarct scar ultrastructure was clearly dysregulated compared to wild-type controls, and we hypothesized that this altered the scar mechanical properties, thereby causing severe infarct thinning and expansion [29]. Decorin-null collagen fibrils had a larger range of diameters, and were more loosely packed than their wild-type counterparts. The reason for the disparity between decorin- and biglycan-null scars may lie in the two SLRPs' collagen-binding properties. Decorin and biglycan have been shown to compete for binding sites on type I collagen [103]. Furthermore, the association of decorin with type I collagen produces thinner fibrils, possibly because it inhibits

lateral aggregation during their formation [104]. Together, these data suggest that the removal of biglycan frees additional binding sites for decorin, which then prevents the enlargement of fibril diameter to the extent biglycan would allow.

Collagen type I is the major structural component of the mature infarct scar, and the scar mechanical properties depend on a variety of characteristics of the collagen molecule, fibril organization, and the arrangement of scar fibers [95,148]. It could be expected that tissue with predominantly smaller diameter collagen fibrils may be less stiff, and this has been demonstrated in biglycan/fibromodulin double-knockout patellar tendons compared to the wild-type [99]. However, the data presented in the present study indicate *Bgn*$^{-/0}$ scars were actually stiffer than *Bgn*$^{+/0}$. A greater density of fibrils may have compensated for this. The number of fibrils per unit area was not quantified, but inspection of representative cross-sectional EM images in Figures 2.3A and B shows that greater fibril density is likely in *Bgn*$^{-/0}$ scars.

Collagen fibril organization could be another important factor in the stiffness and integrity of *Bgn*$^{-/0}$ scars. Fibrils of decorin-null scars were loosely packed and disorganized, and significant infarct expansion was observed [29]. Similar disorganization did not occur in *Bgn*$^{-/0}$ scars. Proper fibril orientation may be required for the scar to withstand the deformations imposed by the cardiac cycle. Holmes and colleagues found that fibril orientation is an important factor in the strain distribution of infarct scars—the largest fibrils were found in the direction of smallest strain [95]. Since there was no apparent disruption of fibril organization in *Bgn*$^{-/0}$ scars, their integrity was likely maintained.

In contrast to the decorin-null, *Bgn*$^{-/0}$ infarcts did not expand compared with the wild-type, and may have even expanded less. This could be related to the stiffness of the scar. Models have shown that stiffer scars can restrict systolic stretching [149], while compliant scars have more negative effects on systolic function [150]. These data suggest stronger infarct tissue may be less affected by the stresses that lead to infarct expansion and remodeling. The change in infarct size from day 1 to day 30 post-MI was twice as large in the *Bgn*$^{+/0}$ as the *Bgn*$^{-/0}$, but the difference was not statistically significant. However, because of the variability in infarct size that is common in MI studies, it would be extremely difficult to show a difference without a method of measuring infarct size in the same animals at different time points, such as delayed contrast-enhanced magnetic resonance imaging, even by increasing the number of animals.

Fibrosis of the remote LV is another important component of post-MI ventricular remodeling. Global ventricular collagen deposition is commonly observed with the increase in wall stress resulting from pressure overload and MI. An increase in biglycan expression has been reported in animal models of both pathologies [36,151]. In an aortic banding study, banded rats with carotid pressures of 162 ± 3 mmHg compared to 133 ± 4 mmHg in sham-operated rats showed increased expression of biglycan by fibroblasts [151]. Rats in heart failure as a result of MI showed global cardiac induction of biglycan, which the authors hypothesized may have enhanced TGF-β activity and increased collagen deposition [36]. They also presented evidence that Angiotensin-II induces biglycan in heart failure, and that this induction can be blocked with an AT1 receptor antagonist, a drug known to slow pathological remodeling. These findings

support the trend toward the reduced remote collagen concentration observed in *Bgn*$^{-/0}$ left ventricles. Ventricular wall stress may not have reached the level present in heart failure, which could explain the lack of statistical significance. This potential for attenuated global cardiac collagen deposition may confer a functional advantage to *Bgn*$^{-/0}$ hearts and delay the onset of failure, mimicking the therapeutic actions of AT1 antagonists. In fact, increased liver weight, a manifestation of the systemic congestion that is a hallmark of heart failure, was observed in *Bgn*$^{+/0}$ but not *Bgn*$^{-/0}$ mice 30 days post-MI. Further study will be necessary to discover if heart failure is actually postponed in *Bgn*$^{-/0}$ mice.

In this report, we show for the first time that null expression of the SLRP biglycan is associated with altered collagen ultrastructure and mechanical properties in the mature post-MI scar. This model may also provide a novel avenue for studying the relationship between scar mechanics and the possibility of delayed onset of heart failure.

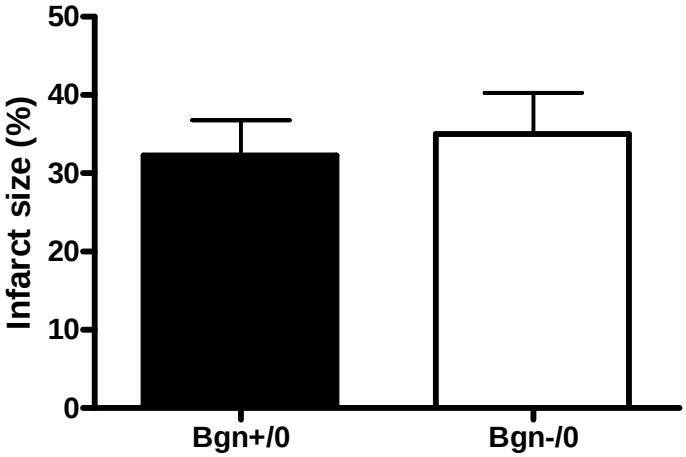

Figure 2.1: One day following MI, infarct size as measured by TTC staining was not significantly different between genotypes ($Bgn^{+/0}$: n=7, $Bgn^{-/0}$: n=9, P=0.6).

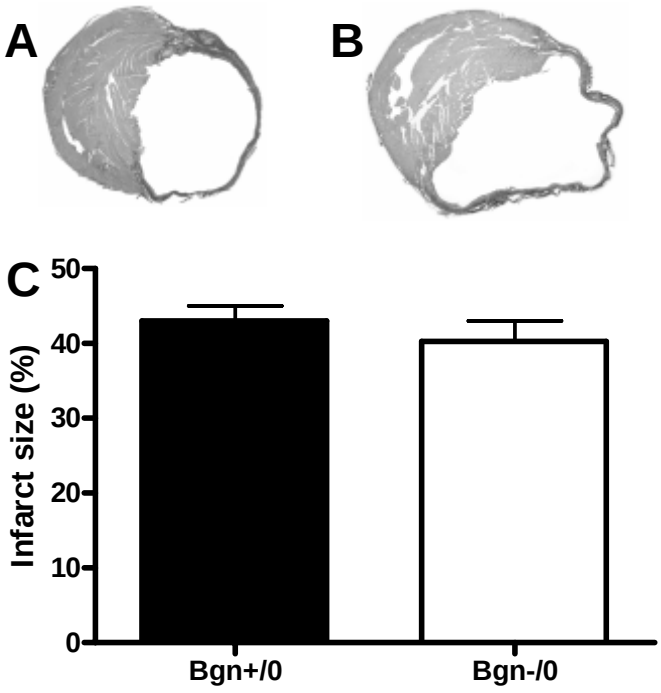

Figure 2.2: 30 days after MI, scar size is similar between genotypes. Representative micrographs of $Bgn^{+/0}$ (A) and $Bgn^{-/0}$ (B) hearts stained with picrosirius red. Infarct size measured from histological sections (C) was not significantly different ($Bgn^{+/0}$: n=7, $Bgn^{-/0}$: n=8, P=0.4).

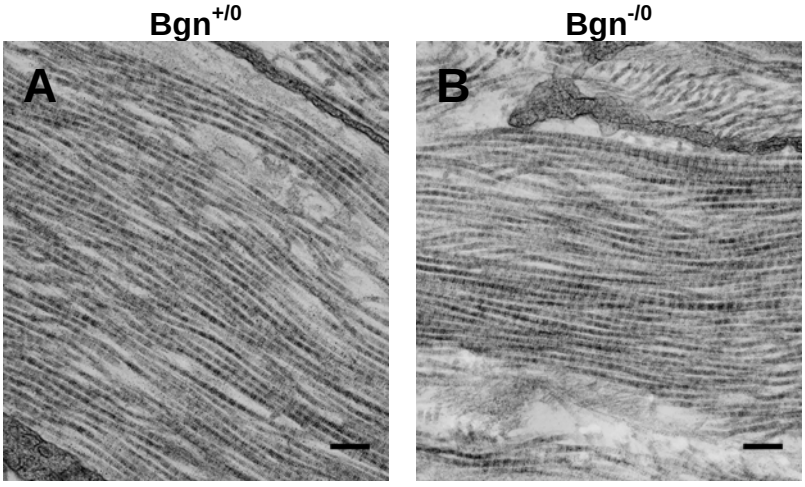

Figure 2.3: There were no apparent differences between genotypes in longitudinal collagen fibril ultrastructure of the scar 30 days post-MI. Representative electron micrographs (20,000×) of *Bgn*$^{+/0}$ (A) and *Bgn*$^{-/0}$ (B); bar=200 nm.

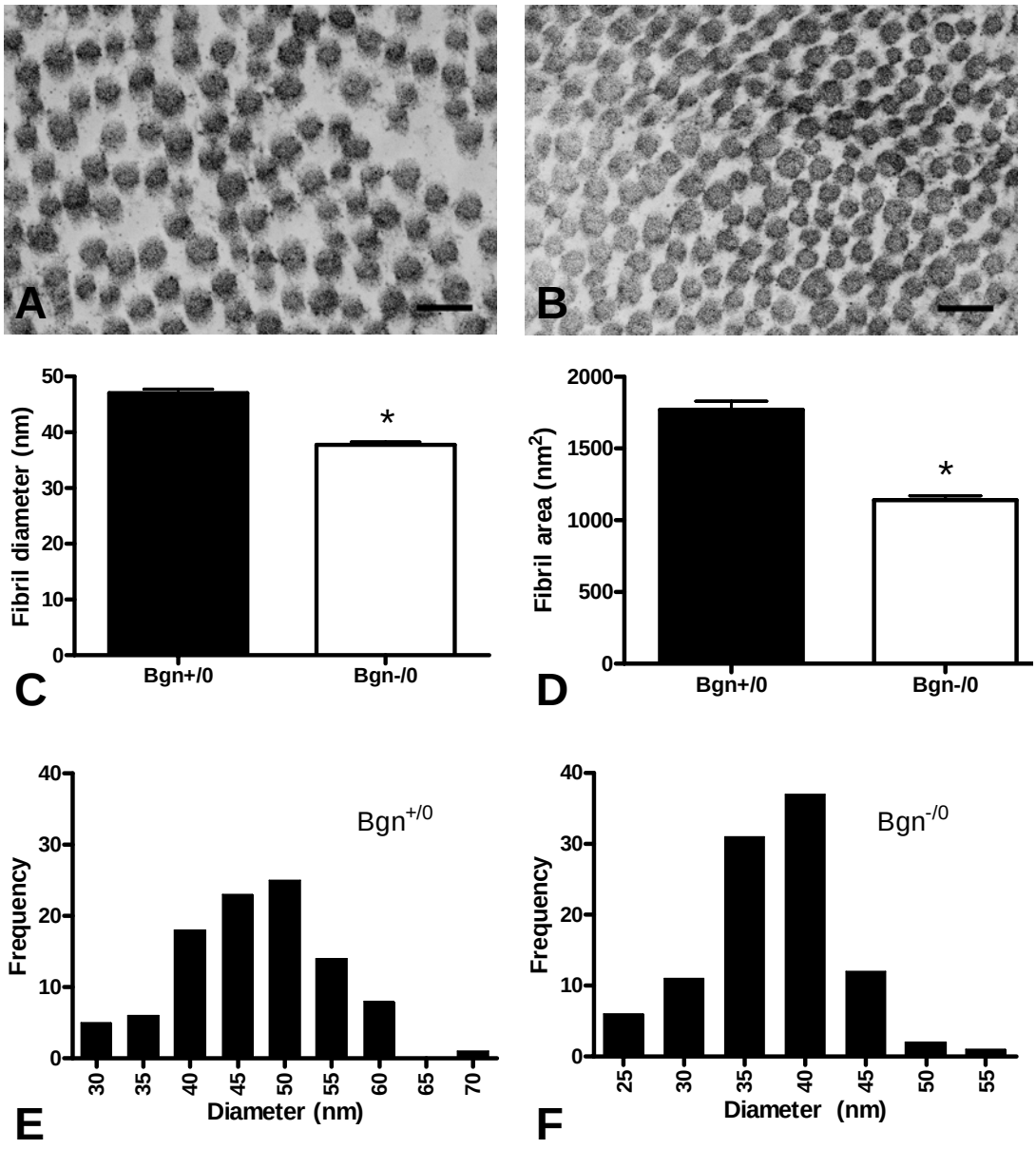

Figure 2.4: Collagen fibril ultrastructure is altered in *Bgn*$^{-/0}$ scars. Fibril diameter (C) and area (D) were significantly smaller in *Bgn*$^{+/0}$ scars compared to *Bgn*$^{-/0}$ (n=100, P<0.0001 diameter and area). Representative electron micrographs (50,000×) of *Bgn*$^{+/0}$ (A) and *Bgn*$^{-/0}$ (B) scars; bar=100 nm. Fibrils appear to be more closely packed in *Bgn*$^{-/0}$ scars. The distribution of fibril diameters was different between genotypes (E, F). The variance in diameter was significantly smaller in *Bgn*$^{-/0}$ scars (F, P<0.005).

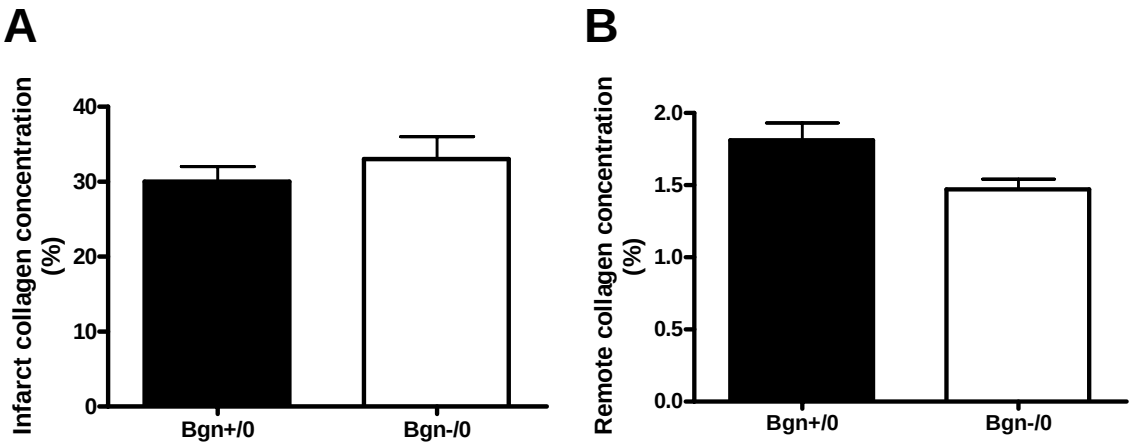

Figure 2.5: Collagen concentration, measured by hydroxyproline content, in the infarct region 30 days post-MI was not significantly different between genotypes (A, $Bgn^{+/0}$ n=6, $Bgn^{-/0}$ n=7, P=0.4). $Bgn^{-/0}$ left ventricles tended to have less collagen deposition in the remote region (B), but the difference was not statistically significant ($Bgn^{+/0}$: n=6, $Bgn^{-/0}$: n=4, P=0.07).

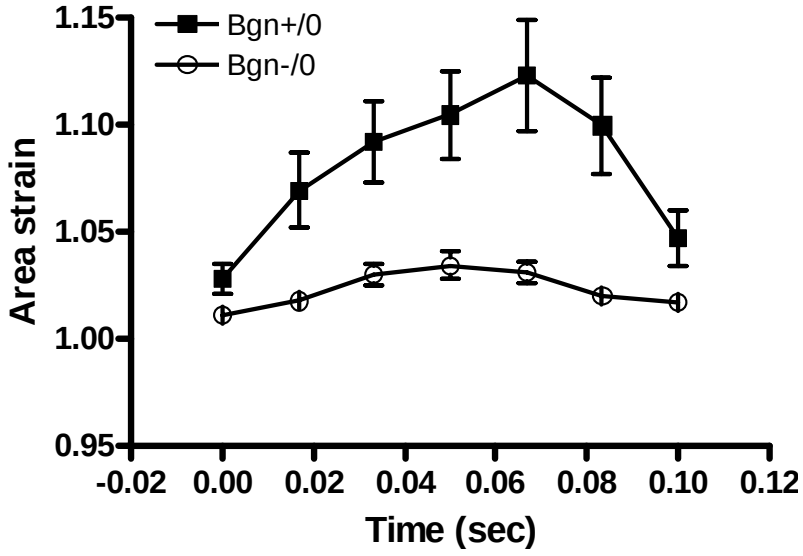

Figure 2.6: Average *in vivo* area strain over the beat cycle, measured by surface markers placed directly on the scar. 4 beats from each of 4 $Bgn^{+/0}$ and 4 $Bgn^{-/0}$ hearts were averaged. Strain was smaller in $Bgn^{-/0}$ scars (P=0.005). The variability in strain was also smaller in $Bgn^{-/0}$ scars.

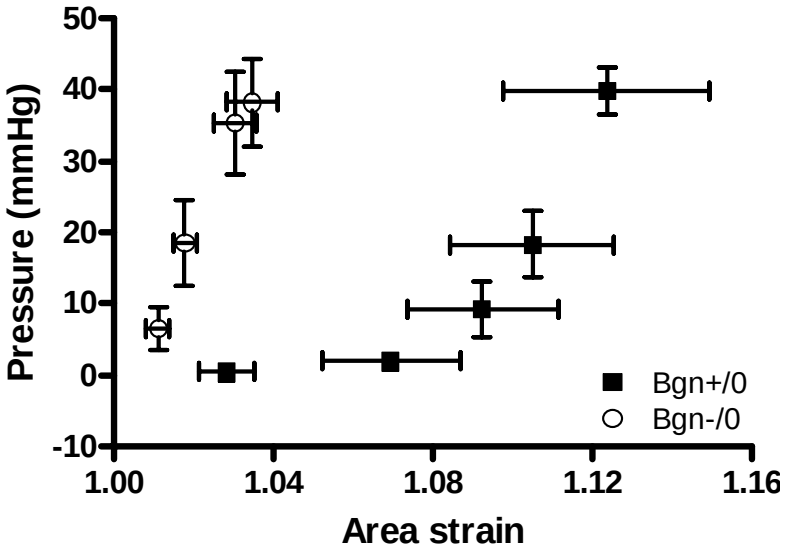

Figure 2.7: Average *in vivo* pressure-strain curves, measured by a conductance catheter and surface markers. 4 beats from each of 4 $Bgn^{+/0}$ and 4 $Bgn^{-/0}$ hearts were averaged. $Bgn^{-/0}$ scars were significantly stiffer (P=0.01).

Chapter 2, in full, is a reprint of the material as it appears in: Campbell PH, Hunt DL, Jones Y, Harwood F, Omens JH, McCulloch AD, *Molecular and Cellular Biomechanics* 5(1):27-35, 2008; copyright Tech Science Press. Used with permission. The dissertation author was one of two primary investigators and authors of this paper.

3 Mechanisms of Increased Acute Post-Myocardial Infarction Survival and Enhanced Chronic Healing in a Murine Model of Myocardial Regeneration

3.1 Abstract

The Murphy Roths Large (MRL) mouse, a strain capable of rapid ear wound healing and right ventricular regeneration, has been shown to survive myocardial infarction (MI) induced by permanent coronary artery ligation at a significantly higher rate than C57BL6/J (C57) controls. We discovered that the great majority of this difference occurs in the first 5 days post-MI. The biological processes responsible for the MRL's acute survival advantage are unknown. To assess the effect of genetic

background, we performed a survival study that included the LG/J strain, which contributes 75% of the MRL's genetic background and is also a rapid ear wound healer. After 5 days, 91% of MRL mice had survived, while C57 survival dropped to 69% ($P < 0.05$). LG/J survival was intermediate at 75% (P = NS). The most common cause of death in C57 and LG/J mice was left ventricular rupture, while MRLs appeared to succumb to pulmonary congestion. After 30 days, survival proportions were 88%, 66%, and 75% in MRL, C57, and LG/J mice, respectively. Because infarct size was similar between the strains after 1 day ($P = 0.67$) and 5 days ($P = 0.97$), the MRL's increased survival relative to the C57 could not be attributed to less severe ischemic injury. To gain mechanistic insight into the difference in survival, we performed a microarray study at acute timepoints. Analysis of microarray data and annotation with Gene Ontology terms revealed a significantly attenuated apoptotic ($P < 0.05$) response in MRL hearts 1 day post-MI compared to the C57, as well as a delay in the expression of stress response transcripts. Supporting the microarray results, there was an 8-fold decrease in TUNEL-positive cells 1 day post-MI in MRL infarcts compared to the C57 ($P < 0.05$). Additionally, there was a 4-fold decrease in the number of CD45-positive inflammatory cells per square millimeter of tissue in the MRL infarct border zone ($P < 0.01$). Chronically, MRL hearts had smaller infarct scars 30 days post-MI than C57 hearts ($P < 0.05$), and attenuated indices of left ventricular dilation and expansion ($P < 0.01$). We conclude that the MRL's early post-MI survival advantage over the C57 is mediated at least in part by reductions in apoptosis and inflammatory infiltration, and that this may influence chronic remodeling. The LG/J's intermediate survival rate

suggests the MRL's high tolerance for MI may be derived from its shared genetic background with the LG/J, but the absence of ventricular rupture may be indicative of additional pro-survival mechanisms at work in the MRL.

3.2 Introduction

Heart disease remains the leading cause of death in the industrialized world, with myocardial infarction (MI) as one of its major causes. Because of the cardiac myocyte's limited self-renewal capability, wound repair consists largely of replacing necrotic myocardium with collagenous scar tissue [4,5]. Early complications can include pump failure and myocardial rupture, the latter accounting for up to 10% of acute mortality [6]. Chronically, large infarcts cause progressive ventricular dilation [7], leading the heart into a "vicious cycle" of decompensation and eventual failure.

In contrast to this mammalian paradigm of post-MI healing, urodele newts and zebrafish can completely regenerate cardiac tissue after amputation of the ventricular apex [109,110]. This is accomplished by adult cardiac myocytes that re-enter the cell cycle and proliferate into the wounded area [109,110]. Though recent evidence has pointed to the existence of a cardiac progenitor cell population in mammals [112-114,119], including humans [152], without intervention such as delivery of growth factors [118] very little renewal occurs [3].

The MRL mouse has emerged as an intriguing, if somewhat controversial, model to study regenerative cardiac healing. Now bred as a wildtype control for the lymphoproliferative MRL-*Fas*^{lpr}, the MRL/MpJ was generated through a series of

crosses with LG/J (75%), AKR/J (12.6%), C3H/HeDi (12.1%), and C57BL/6J (0.3%) [153]. Its potential for regenerative healing was discovered when through-and-through ear hole punches used for colony marking healed rapidly and closed fully within 30 days, with complete replacement of normal tissue architecture [122]. The LG/J shares this fast-healing trait, though ear punch wounds do not close completely [154]. Leferovich et al. [123] were the first group to report that MRL mice are capable of regenerating right ventricular (RV) myocardium after cryoprobe injury. Subsequent studies have both reproduced this result [155] and failed to observe regeneration [128,129]. Several groups tested the MRL's response to a more severe myocardial injury in the form of MI, either by ischemia/reperfusion [126] or permanent coronary ligation [125,127-129,155]. In contrast to RV cryoinjury, complete regeneration of left ventricular (LV) myocardium was not observed. However, Naseem et al. [155] reported the presence of myocytes undergoing cell division in the infarct border zone, as well as significantly increased chronic survival compared to C57BL/6J (C57) controls. The reasons for this difference are unknown.

The purpose of the present study was to elucidate the biological processes responsible for the MRL's increased post-MI survival, and to investigate whether its major genetic background, the LG/J, also displays heightened survival and healing traits. Here we show that the MRL's increased acute survival results from the absence of ventricular rupture, and may be a consequence of decreased apoptosis and inflammatory infiltration compared to the C57. The LG/J is also susceptible to rupture, but survives at a rate between the C57 and the MRL. Chronically, MRL hearts heal with

reduced infarct scar size and indices of LV dilation and infarct expansion compared to C57s.

3.3 Methods

3.3.1 Animals and Surgery

Male C57BL6/J, MRL/MpJ, and LG/J mice were obtained from the Jackson Laboratories and housed in a vivarium according to institutional guidelines. Animals were between 15 and 21 weeks old at the time of surgery. All animal studies and husbandry were conducted under approved University of California, San Diego Animal Subjects Protocols in AAALAC-approved facilities.

Coronary artery ligation surgery was performed as described previously [108]. Briefly, animals were intubated, mechanically ventilated, and left thoracotomy was performed under isoflurane anesthesia. Buprenorphine (0.1 mg/kg) was given after intubation as a post-operative analgesic. After retracting the pectoralis muscles, the heart was exposed through the third intercostal space, the pericardium was retracted, and the left coronary artery was ligated with a 7-0 silk suture. The appearance of paleness distal to the suture confirmed ischemia. The lungs were overinflated, the ribs closed, and the pectoralis muscles returned to their original position. Skin incisions were closed with tissue glue (VetBond, 3M). Animals were rehydrated with warm saline, removed from the ventilator, and allowed to recover on a water-circulating heating pad with access to oxygen. After regaining consciousness, mice were

transferred to a clean cage and monitored for signs of distress. An additional dose of buprenorphine was given the following day if indicated.

3.3.2 Survival studies

The MI procedure described above was performed on C57, MRL, and LG/J mice. Subsets of all three strains that were sacrificed after 1, 2, 5, or 30 days became censored subjects in a Kaplan-Meier survival analysis. Deaths were recorded on a daily basis. Subsets of the day 30 post-MI groups and non-operated controls were continuously administered 1% 5-bromo-2'deoxyuridine (BrdU, Sigma) *ad libitum* in the drinking water.

3.3.3 Initial infarct size

Animals were anesthetized with isoflurane as described above, and maintained at 5% to ensure deep anesthesia. A thoracotomy was performed, the heart was removed, and immediately immersed in an ice-cold, hyperkalemic Krebs-Henseleit buffer containing 2, 3, 5-butanedione monoxime (BDM, Sigma) to stop beating and delay contracture. Hearts were rinsed in fresh buffer, trimmed of collagenous adhesions, and photographed. The atria were removed and weighed, and the ventricles were weighed after removal of the great vessels at the base. The right ventricle was trimmed away, and the left ventricle (LV) was wrapped in plastic wrap or foil and placed in a –20°C freezer for 1-2 hours. The LV was cut into slices 1 mm thick using a cutting fixture with evenly spaced slits, and the slices were incubated in buffered 2,3,5-triphenyl tetrazolium

chloride (TTC, Sigma) at 37°C for 20 minutes, agitating frequently. The slices were then fixed in 10% zinc formalin (Electron Microscopy Sciences) and stored in PBS. Using this technique, viable myocardium stains dark red, while the unstained infarct region remains pale. Slices were pressed between two plastic plates spaced 1 mm apart with glass slides, and the entire apparatus was submerged in water to fill the space between the slices, enabling clearer imaging. Slices were imaged on both sides with a Coolpix 4500 camera and a Leica MZ6 stereomicroscope. Using ImageJ, the infarct and non-infarct areas were measured for both sides of each slice and averaged. Infarct size was expressed as the ratio of total infarct area to total non-infarct area.

3.3.4 Histology and immunohistochemistry

Hearts were harvested as described above, and the ventricles were left intact. Ventricles were either fixed in 10% zinc formalin for 24 hours and embedded in paraffin, or fresh frozen in Optimal Cutting Temperature compound (OCT, Tissue-Tek) in 2-methylbutane cooled by dry ice. Fixed hearts were processed in graded ethanols, embedded in paraffin, and sectioned at 10 μm. For hearts isolated on day 2 post-MI, 10 μm sections were obtained at the midventricular level and immunohistochemically stained for CD45 to quantify inflammatory cell infiltration [20]. Sections were dewaxed and microwaved for 10 minutes in citrate buffer. Endogenous avidin/biotin and peroxidases were blocked, and a biotinylated mouse anti-CD45 (BD Biosciences) was applied at a 1:100 dilution. CD45 staining was detected with streptavidin-horseradish peroxidase and AEC substrate. Nuclei were counterstained with hematoxylin. Stained

sections were observed under brightfield illumination at ×400 (Zeiss Axio Observer.D1), and 6-7 non-overlapping images covering both infarct border regions for each heart were obtained (AxioCam HRc with AxioVision software). Blinded observers counted the number of $CD45^+$ cells in each image. The area of tissue in each image was calculated by first performing a Gaussian blur with a radius of 2 to eliminate speckling, then separating the image into RGB channels and thresholding the blue channel using Image J. Data from the 3 hearts were averaged for each strain, and reported as the number of $CD45^+$ cells per mm^2 of tissue.

3.3.5 Detection and quantification of BrdU incorporation

Frozen hearts from the animals administered BrdU were stored at –80°C until needed, then sectioned at 5 μm for immunolabeling. Midventricular sections were stained using the BD BrdU *In Situ* Detection Kit according to the manufacturer's instructions. Nuclei were counterstained with hematoxylin. 6 images covering the infarct border regions were acquired at ×400 as above from each heart. BrdU-positive nuclei in each image were counted using ImageJ and averaged over the 6 images per heart to obtain the number of BrdU-positive cells per ×400 field.

3.3.6 Infarct size quantification and morphometric measurements

For hearts isolated on day 5 or day 30 post-MI, 8-10 evenly spaced sections from apex to base were stained for infarct size measurement. Day 5 post-MI hearts were stained with H&E or Masson's trichrome, and day 30 post-MI hearts were stained with

Masson's trichrome. Infarct size was determined using a method modified from Pfeffer et al. [5]. Endocardial perimeters of the infarct and non-infarct regions were measured for each section using ImageJ and multiplied by the section's distance from the apex, yielding infarct and non-infarct areas for each slice. Infarct size was expressed as a ratio of the sum of infarct areas to the sum of non-infarct areas over all slices. Infarct thickness was measured for day 5 and day 30 post-MI hearts; LV dilation and infarct expansion indices [156,157] were also calculated for the day 30 post-MI hearts. Infarct thickness was measured at 3 locations across the scarred LV wall in each of 2-3 sections 1-2 mm from the apex, and averaged. The LV dilation index was calculated as the ratio of LV cavity area to total LV area in one section 1.6-1.8 mm from the apex, near midventricular level. The infarct expansion index was defined as the LV dilation index multiplied by the ratio of the septal wall thickness to the infarct thickness.

3.3.7 Apoptosis detection and quantification by TUNEL assay

24 hours after MI, mice were sacrificed and the hearts frozen in OCT as described above. The day before the staining procedure, 5 μm sections were cut at the mid-papillary level and allowed to dry overnight. Apoptosis detection was performed the following day by a Terminal deoxynucleotidyl Transferase (TdT) dUTP Nick End Labeling (TUNEL) assay (CardioTACS *In Situ* Apoptosis Detection Kit, R&D Systems) according to the manufacturer's instructions. Sections were slightly overstained with Nuclear Fast Red so that cell morphology was visible. Stained sections were observed at ×400 under brightfield illumination, and 20-23 randomly chosen, non-

overlapping images covering the infarct and border regions were acquired. Blined observers counted the number of TUNEL-positive nuclei and TUNEL-negative nuclei in each image. Only those TUNEL-positive nuclei closely associated with myocytes were counted. An apoptotic index, expressed as percent TUNEL-positive nuclei to total nuclei, was calculated for each heart by dividing the sum of TUNEL-positive nuclei in all images by the sum of total nuclei in all images. Once all images were analyzed, apoptotic indices for C57 and MRL mice were compared.

3.3.8 Gene expression analysis with MOE430A microarrays

Animals were anesthetized with isoflurane as described above, and a thoracotomy was performed. The heart was removed and arrested, and the right ventricle was quickly dissected away. A cut through the posterior septal wall enabled the LV to spread flat, and the infarct (including the border zone) and non-infarct areas were carefully separated using a 6mm biopsy punch. Tissue pieces were separately snap-frozen in liquid nitrogen and stored at -80°C. Total RNA was isolated by Berlex Biosciences (Richmond, CA; now Bayer HealthCare Pharmaceuticals) and shipped to Expression Analysis, Inc. (Durham, NC) for hybridization to Affymetrix MOE430A microarrays. Affymetrix Microarray Suite 5.0 was used to generate .cel files.

3.3.9 Comparisons, statistical analysis and HOPACH clustering

Affymetrix .cel files were quality controlled with R (www.r-project.org) packages available from the bioconductor [158] website (www.bioconductor.org). We

used the affyQCReport to quality control arrays and determined that two arrays corresponding to a C57 control infarct and a C57 control non-infarct had large hybridization anomalies, so these samples were excluded from subsequent normalization and analysis. All other sample groups had 4 experimental replicates. To generate $\log_2$ expression signal values, we used the gcRMA package [159]. We then generated two separate sets of moderated *F*-statistics [160] with the limma package to determine if genes were differentially expressed (i.e., had significant interaction *P* values) between C57 and MRL samples in the infarct or the non-infarct regions across the time course (0, 1, and 5 days post MI). Limma uses linear models to analyze expression datasets [160]. We filtered the data set for interaction $P < 0.05$ in either the infarct or the non-infarct regions (1005 probe sets) and at least a 50% fold change in any comparison of baseline to post-infarct time for each genotype (MRL, C57) for each region (infarct, non-infarct), including baseline expression differences between the two mouse lines (739 probe sets). These were filtered to remove duplicate gene symbols (688 probe sets), and were then clustered using the HOPACH clustering algorithm [161].

3.3.10 MAPPFinder results

Second-level clusters obtained using the HOPACH algorithm were annotated with Gene Ontology (GO) terms (www.geneontology.org) using the MAPPFinder program [162]. These results were filtered to include terms with at least 3 changed genes and a Z score of 2 or greater (approximately equivalent to $P < 0.05$). Groups of parent-

child relationships were identified and reduced so that only the term with the highest Z score is reported.

3.3.11 Real-time quantitative RT-PCR

Isolated hearts with and without MI were separated as described above, and infarct and non-infarct areas were stored separately in RNALater (Qiagen). Total RNA was isolated using the RNeasy Midi kit (Qiagen) according to the manufacturer's instructions. cDNA was synthesized from 100 ng of RNA using SuperScript II reverse transcriptase (Invitrogen) according to the manufacturer's instructions. $Oligo(dT)_{12\text{-}18}$ was used as a primer solution. Real-time quantitative reverse transcriptase polymerase chain reaction (qRT-PCR) was performed (Applied Biosystems 7300) using 90 ng of cDNA per reaction well in a final volume of 25 µl, with glyceraldehyde 3-phosphate dehydrogenase (GAPDH) as an internal control. Primer/probe sets were obtained from Applied Biosystems. Fold induction or repression was calculated relative to uninjured (day 0) controls of the same strain and region after adjusting for GAPDH expression, using the comparative Ct (ΔΔCt) method: ΔΔCt = [Ct(gene of interest, MI) - Ct(gene of interest, control)] – [Ct(GAPDH, MI) – Ct(GAPDH, control)], and fold change = $2^{-\Delta\Delta Ct}$ [163].

3.3.12 Statistics

Data were analyzed using GraphPad Prism 4 software. Survival curves were generated according to the Kaplan-Meier method, and a logrank test was used to check

for differences between strains. Data including 3 or more groups were analyzed by one- or two-way ANOVA and Tukey or Bonferroni post-hoc tests. Two-group analysis was performed using an unpaired, two-tailed t-test. The significance level was set at $\alpha = 0.05$. All data are reported as mean ± SEM.

3.4 Results

3.4.1 Initial infarct size

Infarct size 1 day after surgery, determined by TTC staining, was not different between the strains (C57: 37.5 ± 3.6%, $n = 10$; MRL: 35.6 ± 4.6%, $n = 9$; LG/J: 43.0 ± 5.0%, $n = 3$; $P = 0.67$; Figure 3.1A).

3.4.2 MRL mice have a survival advantage compared to C57 mice

Of the animals that underwent MI surgery, 76% of C57, 84% of MRL, and 36% of LG/J mice had successful MI and were included in a survival study (Figure 3.2 and Table 3.1). Hearts were excluded (17% of total) if the ligature was too close to or too far away from the left atrium when MI was present, or if there was only trace ischemia, indicating unsuccessful ligation. Approximately 8% died during surgery, and about 3% succumbed to respiratory failure within 1 hour of surgery. Of the animals included in the study, 91% of MRL mice had survived after 5 days, while C57 survival dropped to 69% during the same time ($P < 0.05$, Figure 3.2). The major risk period for C57 deaths was between 2 and 5 days post-MI, but most died on days 3 and 4. LG/J survival was intermediate at 75% after 5 days (P = NS). There was a significant trend in survival by

strain ($P < 0.01$). The cause of death in most C57 and all LG/J mice that died during this period was left ventricular rupture, determined by the presence of blood in the chest cavity at necropsy. The site of rupture was sometimes visible as a tear in the myocardium. The few MRLs that died in the first 5 days appeared to succumb to pulmonary edema, diagnosed by the presence of fluid in the lungs. After 30 days, survival proportions were 88%, 66%, and 75% in MRL, C57, and LG/J mice, respectively (Figure 3.2).

In a cohort of animals, we measured infarct size and thickness on day 5 post-MI to determine if the MRL's increased survival could be related to attenuated infarct expansion [42] or preserved thickness compared to C57 or LG/J hearts (Figure 3.1B, C). Hearts from C57 and LG/J mice that died of rupture before day 5 were also included. There were no significant differences in infarct size between groups (C57: 48 ± 7%, n = 5; C57 ruptured hearts: 53 ± 4%, n = 3; MRL: 55 ± 3%, n = 4; LG/J: 48 ± 8%, n = 4; P = 0.86; Figure 3.1B), so the MRL's acute survival advantage could not be attributed to attenuated infarct expansion. There were also no significant differences in infarct thickness between the groups (C57: 0.76 ± 0.12mm; C57 ruptured hearts: 0.50 ± 0.03mm, n = 6; MRL: 0.56 ± 0.05mm, n = 3; LG/J: 0.63 ± 0.05mm; LG/J ruptured hearts: 0.62 ± 0.02mm, n =2; P = 0.17; Figure 3.1C), but some trends were apparent. C57 survivors tended to have thicker infarcts than those that ruptured, but MRL infarcts tended to thin nearly as much as the C57 ruptured infarcts, and there was no difference in infarct thickness between LG/J survivors and ruptured hearts. These trends suggest that infarct thinning may be an important determinant of rupture risk in the C57 but not

in the LG/J, and that the MRL's increased survival cannot be attributed to preserved infarct thickness.

3.4.3 Enhanced reparative response in MRL infarcts

To generate hypotheses regarding which biological processes could contribute to the MRL's increased survival, we analyzed gene expression before (day 0) and 1 and 5 days after MI in the infarct and non-infarct regions of C57 and MRL hearts (n = 3-4 per group), using a total of 48 genome-wide Affymetrix MOE430A microarrays. Out of the >22,000 transcripts represented on the arrays, 688 met our filtering criteria of $P < 0.05$ by a permuted F test and absolute value of fold change greater than 1.5 in any comparison. HOPACH clustering [161] of this group identified nine second-level clusters with characteristic gene expression patterns (Figure 3.3). Cluster 1 encompassed genes with a pattern of repression in the MRL after MI compared to day 0, with weaker repression in the C57, and induction in the MRL on day 0 compared to the C57 (R-MRL cluster). Cluster 2 included genes with a pattern of repression in both MRL and C57 after MI, with stronger early repression in the C57 infarct (R-C57/MRL cluster). Genes in Cluster 3 were progressively repressed in the C57, with little change in the MRL (PR-C57 cluster). Cluster 4 included genes with a pattern of progressive induction in the MRL infarct and non-infarct, with a weaker and later induction in the C57 (PI-MRL cluster). Cluster 5 genes were repressed in the MRL day 1 infarct and induced later (day 5) in the C57 (LI-C57/R-MRL cluster). Cluster 6 genes were unchanged in the MRL and induced late in the C57 infarct (LI-C57 cluster). Cluster 7 genes showed a

pattern of progressive induction in the C57 infarct and non-infarct regions, while induced only slightly in the MRL (PI-C57 cluster). Cluster 8 genes were induced early (day 1) in the C57 infarct and non-infarct regions with a decline on day 5, while the MRL showed a weaker induction on day 1 and slight repression on day 5 (EI-C57/MRL cluster). Finally, Cluster 9 genes showed early induction in the C57 infarct and non-infarct regions (day 1), and repression in the MRL day 1 infarct (EI-C57/ER-MRL cluster).

Using MAPPFinder [162], we annotated the 9 second-level clusters with Gene Ontology (www.geneontology.org) terms (Figure 3.3) to understand the functional significance of the changed genes. The GO terms most closely related to known effects of MI injury appeared in the PI-MRL and EI-C57/MRL clusters (Table 3.2). These clusters had a characteristic set of terms in common that appeared to be related to the MI injury itself, suggesting that some aspects of the reaction to MI are similar in the MRL and the C57, though the pattern of induction was progressive in the MRL and early in the C57. These characteristic terms included "response to stress" ($n = 15$ associated transcripts in PI-MRL, $P < 0.001$ and 11 in EI-C57/MRL, $P = 0.001$) and its children "response to wounding" ($n = 8$, $P = 0.001$ and 5 transcripts, $P = 0.01$, respectively), "immune response" ($n = 12$, $P = 0.001$ and 8 transcripts, $P < 0.01$, respectively), and "inflammatory response" ($n = 4$, $P < 0.05$ and 3 transcripts, $P = 0.05$, respectively). However, there was also clear differential regulation. The EI-C57/MRL cluster contained transcripts associated with "induction of apoptosis" ($n = 3$, $P < 0.05$) and "negative regulation of cell proliferation" ($n = 3$, $P < 0.05$) that were not present in

the PI-MRL cluster. Apoptotic transcripts were also present in the PI-C57 cluster ($n = 3$, $P < 0.05$). In contrast, the PI-MRL cluster contained numerous transcripts related to reparative processes, including those associated with the GO terms, "positive regulation of development" ($n = 4$, $P < 0.001$), "positive regulation of cell differentiation" ($n = 3$, $P < 0.01$), and "cell motility" ($n = 6$, $P < 0.05$); cellular constituents such as "extracellular matrix" ($n = 6$, $P = 0.005$) and "actin cytoskeleton" ($n = 5$, $P < 0.01$); and biological processes such as "angiogenesis" ($n = 3$, $P < 0.05$).

To validate this analysis, we chose three transcripts to quantify with real-time PCR (Figure 3.4). Platelet-derived growth factor beta (Pdgfb), a cell survival factor [164], and chondroitin sulfate proteoglycan 4 (Cspg4), a mediator of cell adhesion and proliferation [165], were members of the PI-MRL cluster. Fas death domain-associated protein (Daxx), a pro-apoptotic factor [166], was a member of the PI-C57 cluster. The expression patterns of these genes using qRT-PCR (Figure 3.4B) were similar to the patterns we observed in the microarray data (Figure 3.4A).

In summary, MRL and C57 hearts both appear to express transcripts associated with a characteristic response to MI injury, but differential regulation is also apparent. MRL hearts may express more transcripts associated with reparative processes, while C57 hearts may express more transcripts associated with deleterious processes such as apoptotic cell death.

3.4.4 MRL infarct tissue is less susceptible to early cell death

To test the hypothesis suggested by our microarray analysis that differential regulation of apoptosis could be a significant factor in the MRL's increased survival, we performed a TUNEL assay 1 day after coronary ligation in C57 and MRL hearts ($n = 3$ for each group; Figure 3.5A, B). We observed an 8-fold decrease in the number of TUNEL-positive cells closely associated with myocytes in the MRL infarct region compared to the C57 (4.3 ± 0.7% vs. 34 ± 8.0%, respectively; $P < 0.05$; Figure 3.5D). We did not observe TUNEL-positive cells in remote LV myocardium or the interventricular septum of either strain (Figure 3.5C), or in uninjured controls (not shown).

3.4.5 MRL hearts have an attenuated inflammatory response

Our microarray analysis results suggested that the MRL inflammatory response could be delayed compared to the C57, due to the progressive pattern of induction in the PI-MRL cluster compared to the EI-C57/MRL cluster. We investigated the inflammatory response in C57 and MRL mice on day 2 post-MI ($n = 3$ for each group) by immunohistochemical staining for CD45, which labels all leukocytes [167]. There was a 4-fold decrease in the number of $CD45^+$ cells in the MRL infarct border zone compared to the C57 (34.5 ± 7.6 vs. 146 ± 20 cells/mm^2, respectively; $P < 0.01$; Figure 3.6).

3.4.6 MRL hearts have smaller infarct scars and attenuated remodeling

To determine if there was a differential chronic response to MI injury between the strains, a subset of MRL, C57, and LG/J mice were sacrificed after 30 days (n = 14, 13, and 2, respectively). The majority of MRL and C57 animals (n = 11 and 10, respectively) were used for mature infarct scar size measurement, while the remainder of the 30-day subset was continuously administered BrdU in the drinking water over the 30-day period in order to study cellular proliferation. Controls were administered BrdU but did not receive MI injury. In the infarct size measurement group, MRL scars were significantly smaller than C57 scars (37 ± 3% vs. 48 ± 3%, respectively; $P < 0.05$; Figure 3.7A, B). Indices of LV dilation (0.30 ± 0.04 vs. 0.50 ± 0.05, respectively; P = 0.01; Figure 3.7C) and infarct expansion (1.59 ± 0.14 vs. 3.00 ± 0.34, respectively; P = 0.001; Figure 3.7D) were also attenuated. There was a trend toward increased scar thickness in the MRL, but the difference did not reach statistical significance (0.23 ± 0.02mm vs. 0.19 ± 0.01mm, P = 0.08, data not shown). In the BrdU group, there was no difference in the number of BrdU-positive cells per field between MRL and LG/J hearts before (14.9 ± 0.9 cells/field, n = 3 vs. 12.2 ± 1.4 cells/field, n = 3, respectively, P = NS; Figure 3.8C, D) or after MI (30.0 ± 4.9 cells/field, n = 3 vs. 35.4 ± 16.9 cells/field, n = 2, respectively, P = NS; Figure 3.8A, B and quantified in D), though MI induced a significant increase in BrdU-positive cells in both strains compared to their uninjured controls ($P < 0.05$). Uninjured C57 hearts had 17.7 ± 2.8 BrdU-positive cells/field

(Figure 3.8D). We were not able to obtain BrdU incorporation data for C57 hearts post-MI, so this strain was excluded from the statistical analysis.

3.5 Discussion

Here we have shown that increased survival in the MRL mouse compared to the C57 was due to the absence of ventricular rupture in the acute phase post-MI, and that its major genetic background, the LG/J, was also susceptible to rupture. Lack of rupture in the MRL could not be attributed to smaller infarct size, increased infarct thickness or attenuated infarct expansion. We performed a microarray study to generate hypotheses that could potentially explain the MRL's survival advantage, and our analysis suggested that even acutely after MI, MRL hearts began to express transcripts associated with wound repair, while C57 hearts expressed transcripts associated with cell death. This was confirmed with PCR and tissue level assays, the latter showing significantly fewer TUNEL-positive cells as well as less $CD45^+$ inflammatory infiltration in the MRL infarct. Chronically, MRL infarct scars were smaller than C57 scars 30 days post-MI, which could not be attributed to attenuated infarct expansion.

Numerous researchers have reported the presence of ventricular rupture in the C57BL/6J inbred strain during the first week after permanent coronary occlusion [8,20,21,27,39,40,168], which our results reproduced. Infarct thinning in the C57 appeared to be an important determinant of the likelihood of rupture, since survivors on day 5 tended to have thicker infarcts than those that died of rupture. This was not true in the MRL since those infarcts thinned to a similar degree without rupturing. To determine the

uniqueness of the MRL's survival trait, we searched for reports on rupture rates in other inbred strains. Gao and coworkers [27] studied the strain-and gender dependence of rupture in FVB/N, C57BL/6J, and 129sv mice. In male mice, rupture rates were 3%, 27%, and 59%, respectively. These results suggest that rupture is a common acute complication of MI in mice, and its rate is strain-dependent. Although the FVB/N rupture rate was just 3%, this strain was quite susceptible to acute heart failure; 45% of males died from this complication in the first 7 days. Based on these results, the male MRL's acute death rate of 9% reported here is remarkable. However, the presence of a significant trend in survival from the MRL to the LG/J to the C57 in the present study suggests that the MRL's survival trait may be derived in part from the genetic background it shares with the LG/J. Wound healing in the LG/J has been analyzed in a study comparing ear punch healing in 20 inbred strains of mice, including the MRL and the C57 [154]. Both the LG/J and the MRL displayed rapid wound healing kinetics, with the 2mm hole beginning to close quickly after 5 days and reaching complete or nearly complete closure by 30 days. In contrast, C57 wounds still had a diameter of slightly less than 1mm after 30 days. These results suggest that the LG/J could contribute some of the MRL's fast-healing genes. To our knowledge, the present study is the first to examine the LG/J's cardiac phenotype. That theLG/J is susceptible to rupture post-MI while the MRL is not implies there may be additional pro-survival mechanisms at work in the MRL.

Because the MRL's increased survival was likely to be a complex trait, we performed a microarray study at times before (day 1) and toward the end (day 5) of the

risk period of C57 deaths, and compared gene expression in the infarct and non-infarct regions of MRL and C57 hearts to uninjured (day 0) tissue from the same area. Upon clustering and annotating the significantly changed transcripts with GO terms, we found both co-regulation and differential regulation. MI appeared to induce a characteristic response in both MRL and C57 infarcts, described by GO terms such as "response to stress," that might be delayed in the MRL compared to the C57. However, C57 hearts expressed transcripts associated with apoptosis, while MRL hearts expressed transcripts associated with wound repair.

To investigate these results at the tissue level, we first performed a TUNEL assay 1 day post-MI and observed an 8-fold decrease in the number of TUNEL-positive cells closely associated with myocytes in the MRL infarct compared to the C57 infarct. It is currently unknown whether apoptosis contributes to rupture after permanent coronary occlusion. However, a new study investigating the effect of EPO administration after permanent occlusion in C57 mice [169] reported a significant reduction in TUNEL-positive myocytes 2 days post-MI in EPO-treated mice, as well as significantly increased survival compared to saline-treated mice. The bulk of the difference in survival occurred during the first 6 days. The percentage of TUNEL-positive myocytes in saline-treated animals was comparable to that we found in the present study ($37.8 \pm 2.2\%$ vs. $34.0 \pm 8.0\%$, respectively), and agrees with previous reports [26,54].

Next, we performed immunohistochemical staining for CD45 on day 2 post-MI, to determine if the delay in the induction of stress response transcripts suggested by the

microarray data would lead to a difference in inflammatory infiltration. Indeed, there was a 4-fold decrease in $CD45^+$ cells/mm^2 in the MRL infarct border zone compared to the C57. Excessive inflammation post-MI has been linked to rupture in mice overexpressing TNF-α [21], and has been observed at the site and time of rupture [20,27]. Depletion of leukocytes has been shown to protect against rupture [20]. Moreover, the neutrophils likely to compose the majority of the $CD45^+$ cells on day 2 post-MI [8,12,20] are thought to be the source of matrix metalloproteinase (MMP)-9 [8,28,29], which may have a prominent role in degrading the existing ECM and precipitating rupture [8,20]. Though mRNA expression of the cytokines TNF-α and IL-1β were not different between the strains, the potent neutrophil chemoattractant Cxcl7 [170] was strongly induced (48-fold) in the C57 day 1 infarct and not in the MRL. Together, these studies and our data suggest that reduced inflammatory infiltration could contribute to the MRL's increased survival by providing some protection against rupture.

Our data also showed that MRL hearts healed with smaller scars and attenuated remodeling than C57 hearts after MI. The MRL's attenuated scar formation could possibly be derived from the reductions in apoptosis and inflammation early after MI. Reduced acute apoptosis [26,59,60,72,171,172] and inflammation [54,58-60] have been shown to reduce infarct scar size after MI. We did not observe a difference in BrdU incorporation between strains before MI, or between the MRL and LG/J infarct border zones after MI. BrdU-positive myocytes have been observed in the MRL after cryoinjury [123] and MI, [130] but other reports have questioned the presence of BrdU-positive myocytes after MI [128,129], and have not observed a difference in cell proliferation between C57 and MRL

hearts [127-129]. Further study will be needed to determine if any of the BrdU-positive cells in the present study were myocytes.

A number of other groups have studied post-MI healing in MRL mice [125-130]. Our finding of increased acute survival in the MRL confirms and extends that of Naseem and colleagues. [130], who reported a drop in C57 survival after 1 week, and our data provide possible mechanisms of attenuated apoptosis and inflammatory infiltration. However, our chronic healing results diverge from previous studies, which have not found a difference in infarct scar size [126-130]. Two of these used female MRL and C57 mice [127,128]. Because infarct healing is a sexually dimorphic trait [27,173], as are ear punch [174] and cryoinjury [124] healing in the MRL, these studies cannot be directly compared to ours. Another study used ischemia/reperfusion injury, which resulted in an average infarct size of less than 20% [126]. Larger infarct sizes as in the present study may be necessary to observe differential healing in the MRL. Finally, two studies used male MRL mice and permanent coronary occlusion [129,130]. In the first, there was no difference in survival between MRL and C57 mice; both survived about 90% of the time [129]. This high rate of survival in C57 mice is inconsistent with many other studies [8,20,21,27,39,40,168,173], and the only repeated difference appears to be the vendor the animals were purchased from: Harlan [129] vs. Jackson Laboratories [8,20,130,173]. Further investigation would be necessary to determine if there is a difference in post-MI survival between mice of the C57BL/6J strain purchased from different vendors. If rupture is abolished, chronic remodeling could be similarly improved. Finally, Naseem et al. [130] reported a decrease in LV dilation in MRL mice, which is consistent with our

findings, but no difference in infarct scar size. A reason for this could be differing group sizes: $n = 3$ in Naseem et al. vs. $n = 10\text{-}11$ in the present study.

The results presented here lend credence to the idea of the MRL mouse as an intriguing, but complex, model of improved post-MI survival and healing. Our data suggest that these phenotypes could be derived in part from reductions in apoptosis and inflammatory infiltration. The LG/J's intermediate survival indicates that its genetic background could contribute to the MRL's traits. This model could be useful for future studies designed to augment cardioprotection in the mammalian heart.

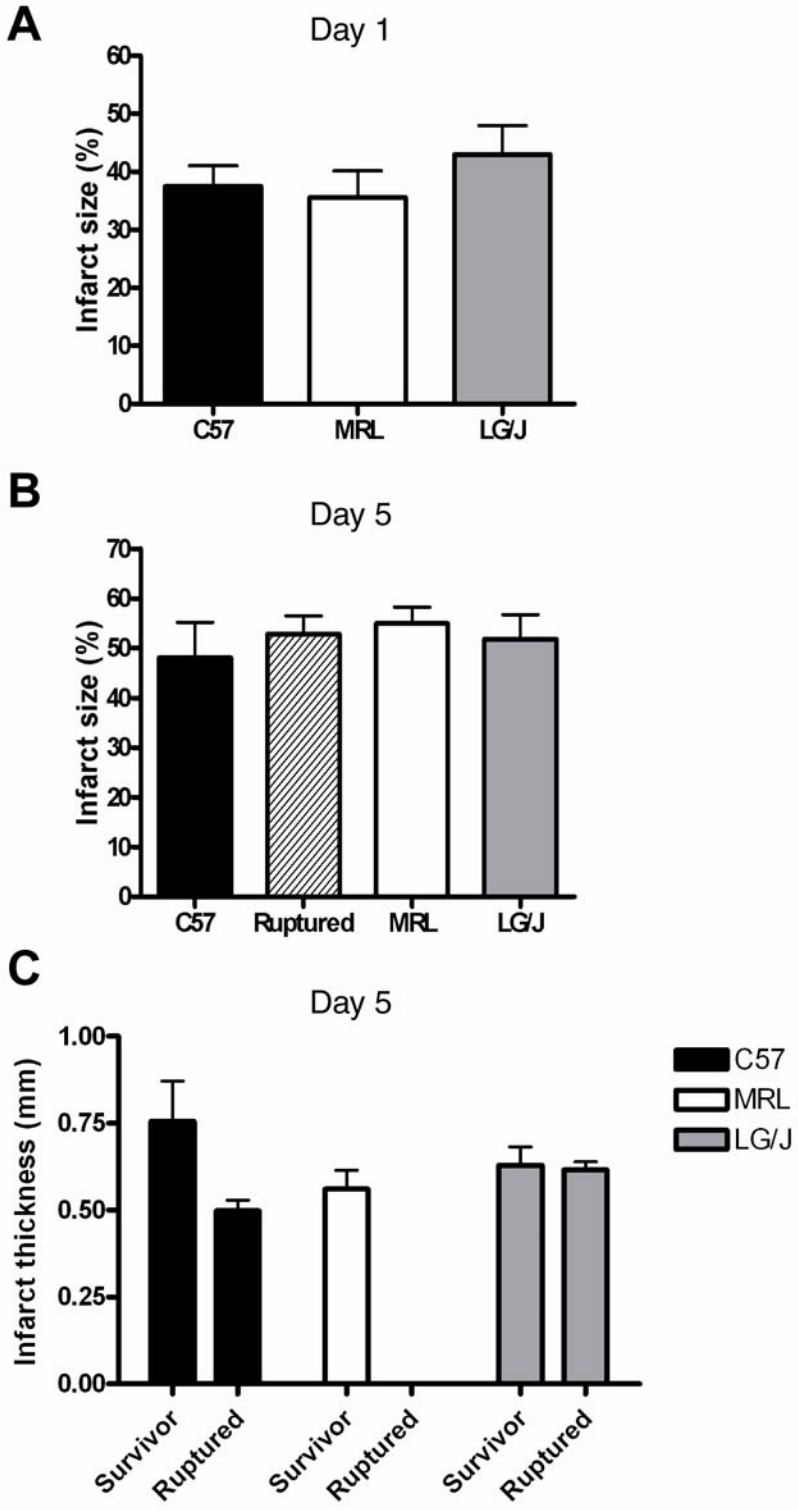

Figure 3.1: A, there was no difference in initial infarct sizes 1 day post-MI in each of the 3 strains. B, infarct size after 5 days in survivors and hearts that ruptured. C, infarct thickness after 5 days in survivors and hearts that ruptured.

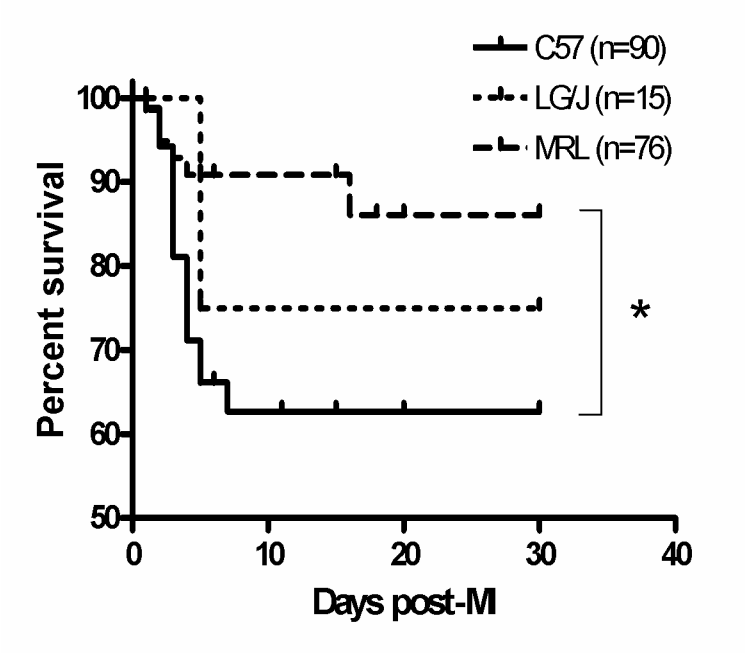

Figure 3.2: Kaplan-Meier survival analysis of all 3 strains through 30 days post-MI. There was a significant trend in survival by strain ($P < 0.01$), and MRL mice survived MI better than C57 mice ($P < 0.05$). There were no differences between the other groups. *, $P < 0.05$.

Table 3.1: Animal numbers for each set of experiments

	C57	MRL	LG/J
Acute mortality (% of total, excluding censored subjects)	21 (34%)	4 (9%)	2 (25%)
Initial infarct size			
24h permanent occlusion	10	9	3
Microarray analysis			
Day 0 infarct, non-infarct	3	4	ND
Day 1 infarct, non-infarct	4	4	ND
Day 5 infarct, non-infarct	4	4	ND
qRT-PCR			
Day 0 infarct, non-infarct	3	3	ND
Day 1 infarct, non-infarct	3	3	ND
Day 5 infarct, non-infarct	3	3	ND
TUNEL staining			
Non-operated	3	3	ND
24h permanent occlusion	3	3	ND
CD45 staining			
Non-operated	3	3	ND
2 days permanent occlusion	3	3	ND
Infarct scar thickness			
5 days permanent occlusion	11 (6 ruptured)	3	6 (2 ruptured)
30 days permanent occlusion	10	11	ND
Infarct scar size			
5 days permanent occlusion	8 (3 ruptured)	4	4
30 days permanent occlusion	10	11	ND
BrdU incorporation			
Non-operated	3	3	3
30 days permanent occlusion	ND	3	2

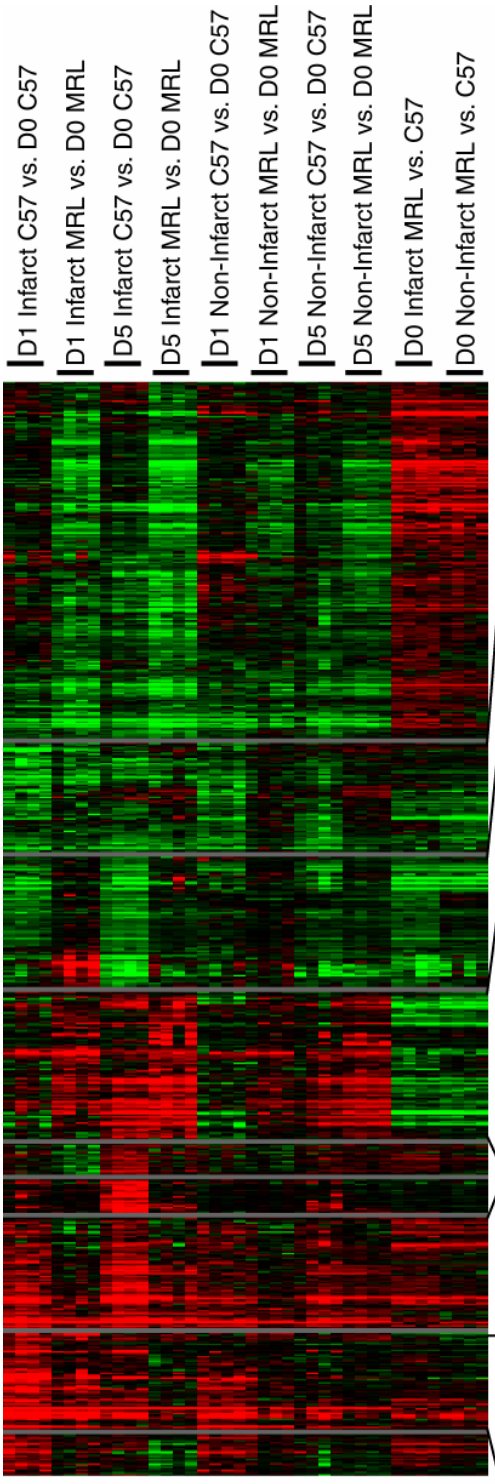

Cluster	GO Term	changed/ measured	Z-score	P
R-MRL				
	Positive reg. of IL-2 biosynthesis	3/9	7.59	<0.001
	Ubiquitin cycle	14/335	3.83	<0.001
	Pos. reg. of T cell proliferation	3/22	4.51	0.004
	Mitotic cell cycle	7/193	2.27	0.036
	Organic acid metabolism	12/417	2.12	0.039
R-C57/MRL				
	GTPase activity	4/131	4.07	0.008
	Transferase activity	12/1211	2.45	0.018
	Kinase activity	7/621	2.19	0.041
PR-C57				
	Regulation of cell migration	3/46	6.17	<0.001
	Cell-substrate adhesion	3/56	5.50	0.001
	Extracellular matrix	5/260	3.59	0.003
PI-MRL				
	Antigen processing via MHC II	3/9	12.10	<0.001
	Positive reg. of development	4/70	5.24	<0.001
	Response to stress	15/837	4.21	<0.001
	Actin cytoskeleton org./biogenesis	5/130	4.51	0.001
	Positive reg. of cell differentiation	3/53	4.50	0.003
	Extracellular matrix	6/260	3.32	0.005
	Cell motility	6/298	2.92	0.018
	Angiogenesis	3/96	2.99	0.034
	Regulation of cell differentiation	3/130	2.33	0.045
PI-C57				
	Integrin-mediated signaling path.	3/59	5.08	0.001
	Cell growth	4/121	4.47	0.001
	Cytoskeleton org. and biogenesis	6/304	3.77	0.003
	Induction of apoptosis	3/143	2.78	0.031
EI-C57/MRL				
	Response to stress	11/837	3.65	0.001
	Protein binding	29/3855	3.10	0.003
	Negative reg. of cell proliferation	3/138	2.90	0.026
	Induction of apoptosis	3/143	2.82	0.035

Figure 3.3: HOPACH clustering and MAPPFinder annotation results. Green, downregulation; red, upregulation. Changed/measured, number of genes in cluster/number on array. Z-score explained in ref. 162.

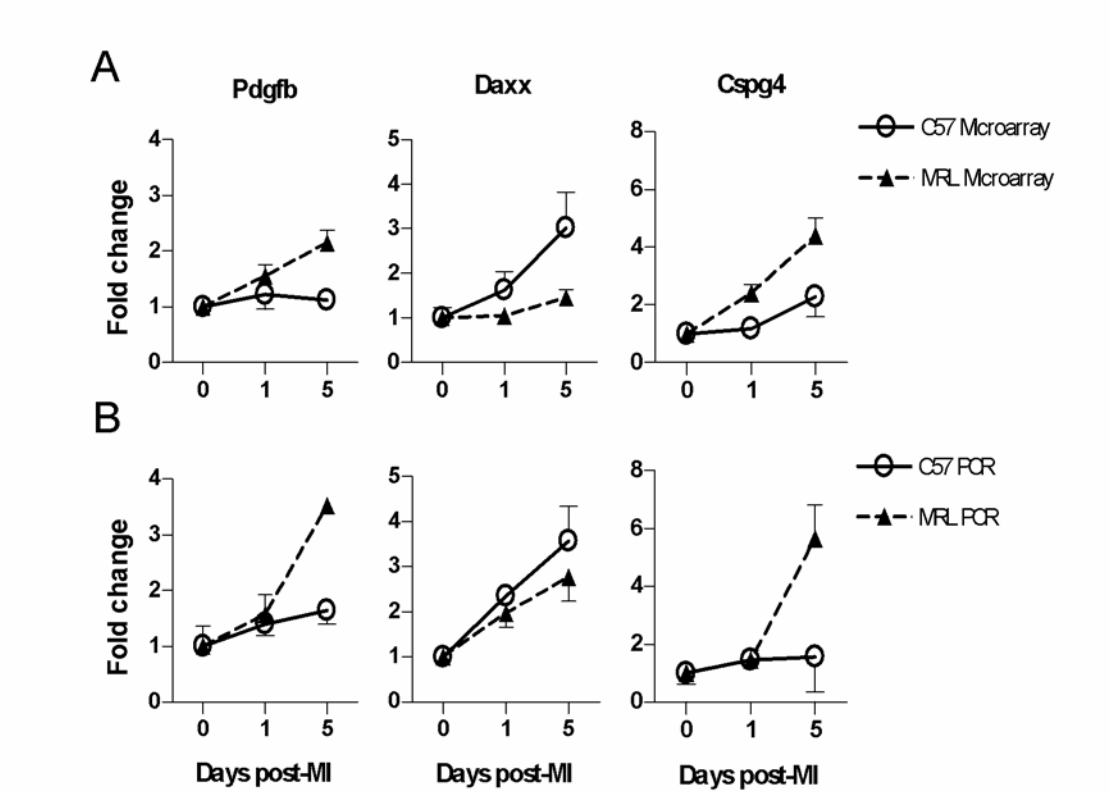

Figure 3.4: Validation of gene expression using Affymetrix MOE430A microarrays (A) with quantitative real-time PCR (B).

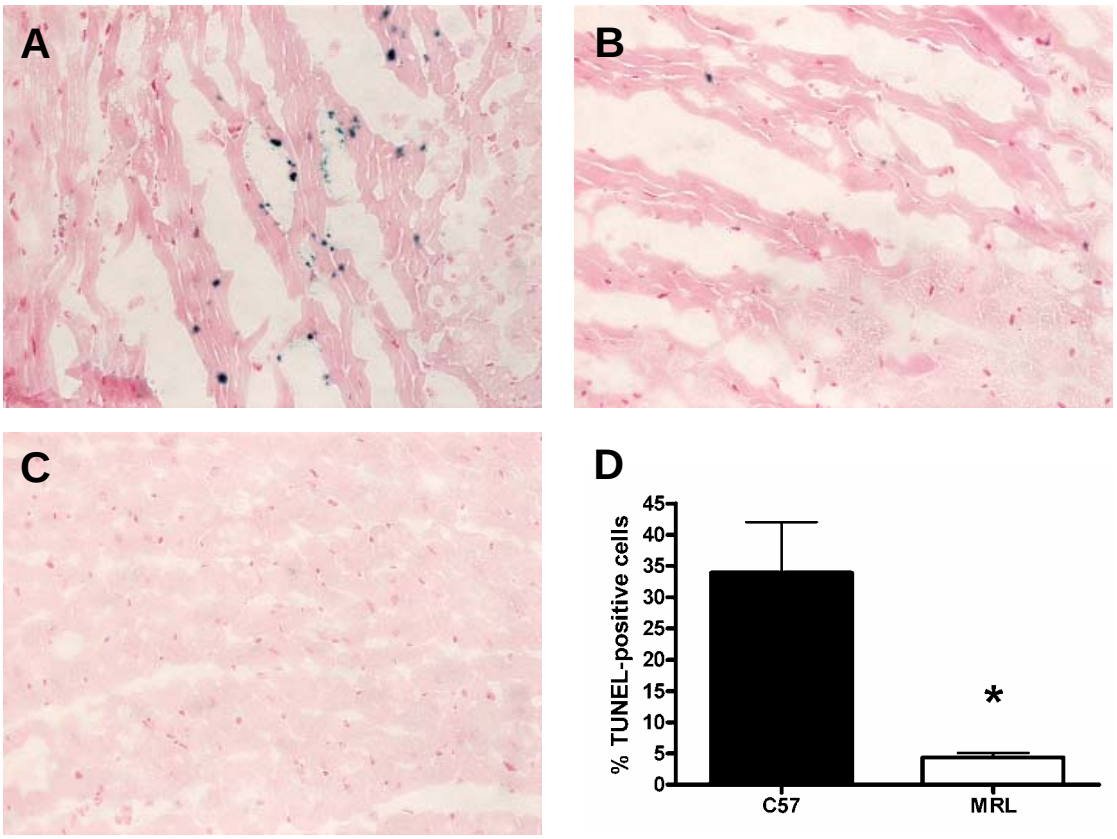

Figure 3.5: TUNEL staining in the infarct border zone of C57 (A) and MRL (B) hearts 1 day post-MI. A representative image of remote myocardium is shown in panel C. D, the number of TUNEL-positive nuclei closely associated with myocytes was significantly higher in C57 hearts than MRL hearts ($P < 0.05$). Magnification ×400. *, $P < 0.05$.

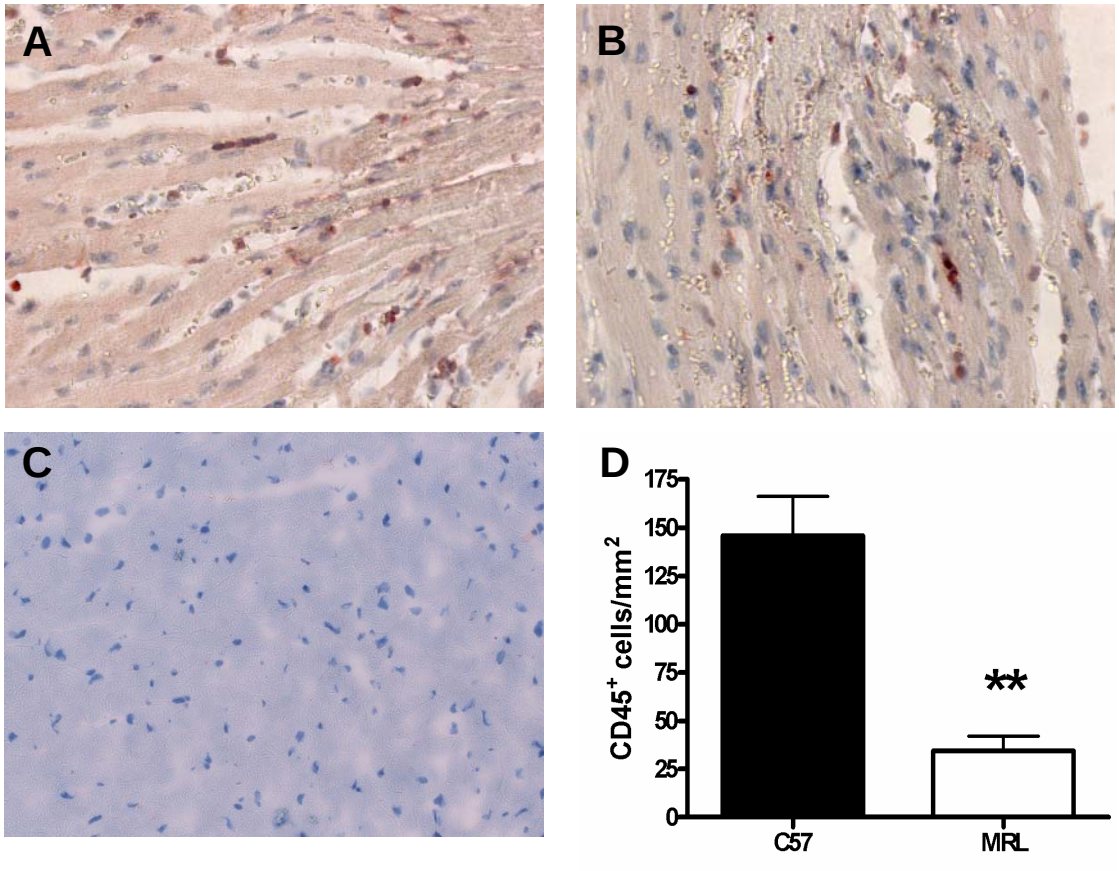

Figure 3.6: CD45$^+$ cells (red) in the infarct border zone of C57 (A) and MRL (B) hearts 2 days post-MI. A representative uninjured control is shown in panel C. D, there were significantly more CD45$^+$ cells per square millimeter in the C57 infarct border zone than in the MRL ($P < 0.01$). Magnification ×400. **, $P < 0.01$.

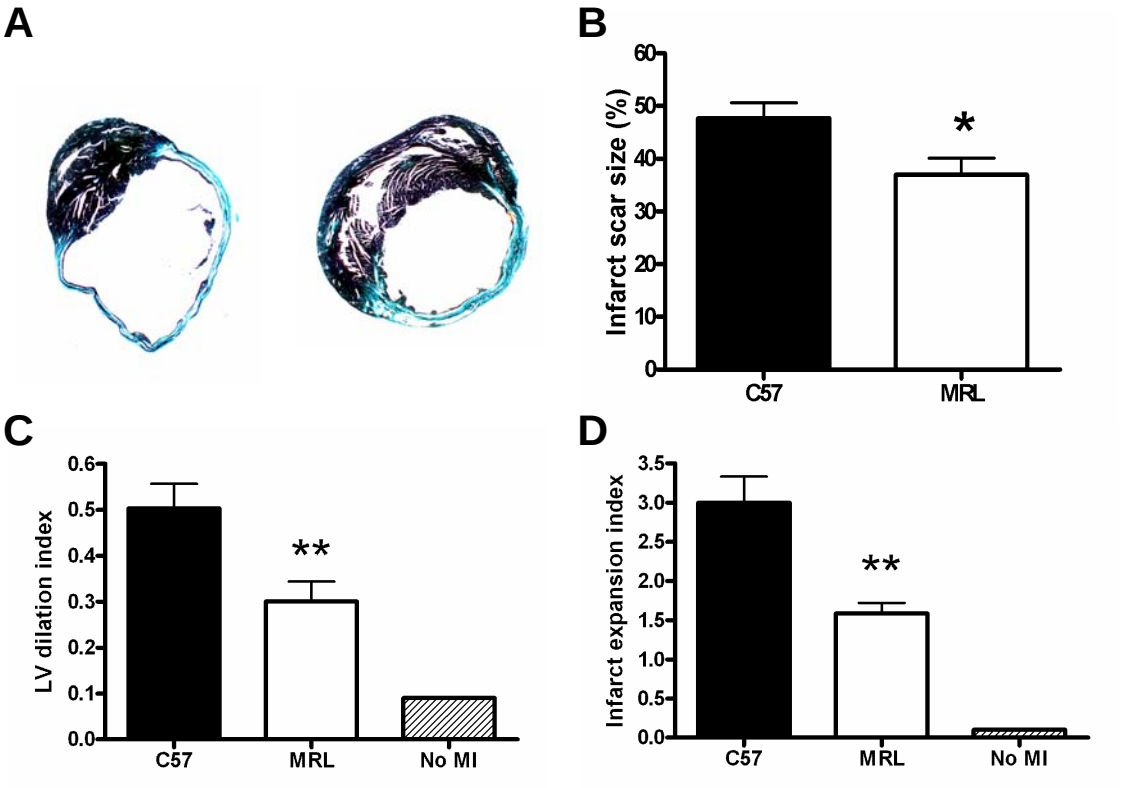

Figure 3.7: Deleterious remodeling in the MRL was attenuated compared to the C57 30 days post-MI. A, representative trichrome-stained sections from C57 (left) and MRL (right) hearts. B, infarct scar size after 30 days was significantly smaller in MRL hearts ($P < 0.05$). LV dilation (C) and infarct expansion (D) were also significantly attenuated. *, $P < 0.05$; **, $P < 0.01$.

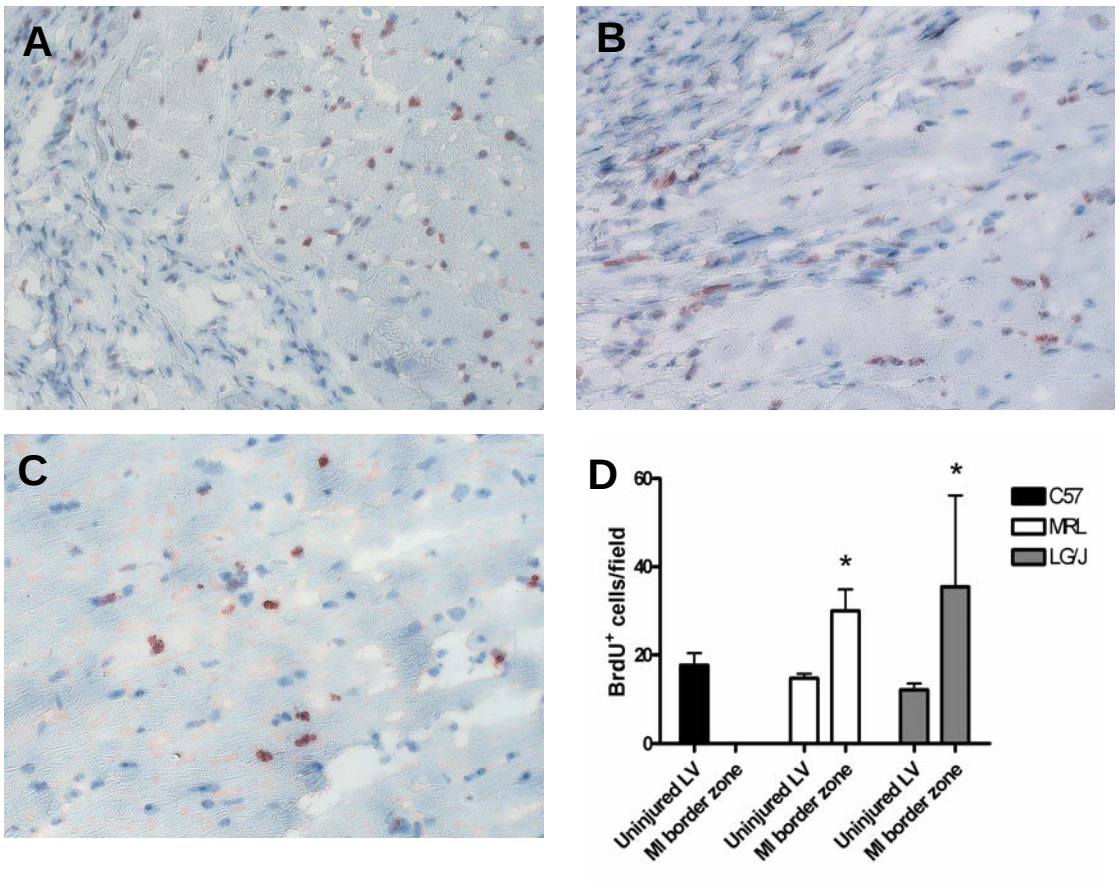

Figure 3.8: There was no difference in BrdU incorporation between MRL (A) and LG/J (B) infarct border zones. Uninjured hearts (representative image in panel C) had significantly fewer BrdU-positive cells than hearts with MI ($P < 0.05$), quantified in D. C57 hearts were excluded from statistical analysis due to the lack of an MI group. *, $P < 0.05$ vs. respective uninjured control.

Chapter 3, in part, will be submitted to the Journal of Molecular and Cellular Cardiology, with authors Hunt DL, Campbell PH, Zambon AC, Vranizan K, Omens JH, McCulloch AD. The dissertation author is the primary investigator and author of this material.

4 Summary and Conclusions

The objective of this dissertation was to investigate the role of abnormal regulation of wound healing in post-myocardial infarction cardiac repair. We studied the effects of deleting an ECM proteoglycan on chronic remodeling, and investigated the mechanisms that could be responsible for heightened acute survival and healing in a model of myocardial regeneration.

4.1 Effects of ECM Proteoglycan Deletion on Post-Myocardial Infarction Remodeling

Proteoglycans of the ECM may regulate the assembly of collagen fibrils, thereby affecting the structure of the collagenous infarct scar. A previous study using mice lacking the proteoglycan decorin [29] had shown that decorin was essential for proper scar formation after MI. The role of other proteoglycans in post-MI healing was unknown.

In Chapter 2, we discussed post-MI healing in mice lacking the small leucine-rich proteoglycan biglycan. We found that biglycan had a significant influence on the formation of collagen fibrils in the infarct scar. Fibrils in biglycan-null scars were smaller, more closely packed, and had a narrower range of diameters than fibrils in wildtype scars. We also found that biglycan scars were stiffer, by constructing pressure-strain curves using *in vivo* measurements of strain on the scar surface. There was no difference in the size of the infarct scar between genotypes, but biglycan-null hearts tended to have less collagen deposition in the surviving myocardium, suggesting that chronic deleterious remodeling could be attenuated. This was supported by data indicating biglycan-null mice had significantly reduced liver weight compared to wildtype mice. We concluded that the biglycan-null mouse might serve as a model of attenuated progression to heart failure, though further study for a longer time period would be needed.

This work contributes to our understanding of the cardiac ECM as a critically important and dynamic structure during post-MI remodeling. Under normal conditions, the ECM facilitates the force transmission that enables the heart to function as a pump [131,132]. Studies have shown that disruption of or discontinuities in ECM components, such as fibrillar collagens, collagen crosslinks, and integrins, may have significant effects on remodeling in the diseased heart [175-177]. These alterations result in myocyte fascicles being subjected to abnormal patterns of stress and strain during the cardiac cycle due to the loss of structural support provided by the ECM, which directly precipitates changes in myocardial geometry and function [31]. More recent evidence has

pointed to a role for proteoglycans in remodeling, as our group previously demonstrated with mice lacking decorin [29]. These mice had severe defects in collagen fibril organization and assembly in the infarct scar, leading to increased ventricular dilation and depressed cardiac function compared to controls. In the present work, we have shown that the lack of biglycan also induces changes in the collagen ultrastructure of the infarct scar, but these changes do not have the same effect as the lack of decorin, and might even delay the onset of heart failure [108]. These studies provide a starting point for understanding the importance of proteoglycans in the cardiac ECM. Future therapies could target ECM proteoglycans such as biglycan by controlling their expression levels to ensure mechanical integrity of the infarct scar.

4.2 Mechanisms of Improved Post-Myocardial Infarction Survival and Healing in the MRL Mouse

Tissue regeneration was once thought to be confined to the limbs of amphibians, but it has been shown that those animals, zebrafish, and recently the MRL mouse are capable of regenerating myocardial tissue. The prospect of heart regeneration in mammals is tantalizing, and research has been undertaken to further investigate cardiac injury in the MRL. The results of this work indicate that the MRL is not capable of completely regenerating myocardium after MI and still heals with a scar, but it survives the MI injury at a greater rate than C57BL/6J controls and may not be as susceptible to deleterious remodeling. Evidence of dividing myocytes has also been presented.

In Chapter 3, we investigated the mechanisms of improved survival and healing in the MRL. We confirmed that MRL mice survive MI significantly better than C57 controls, and that the majority of this difference occurred in the first 5 days post-MI as a result of the absence of ventricular rupture in the MRL. We investigated survival in the LG/J strain, the major genetic background of the MRL, and discovered that it was susceptible to rupture, but had a survival rate between that of the C57 and the MRL. This suggested that the MRL's increased survival may be derived in part from its shared genetic background with the LG/J. To investigate the mechanisms of this improved survival in the MRL compared to the C57, we performed a microarray analysis at acute time points. We discovered that attenuated aopotosis and inflammatory infiltration 1 day after MI were likely to contribute to the MRL's increased survival, and that by day 5 post-MI the MRL expressed transcripts associated with wound repair that were absent in the C57. Chronically, MRL infarct scars were smaller than C57 infarct scars and had attenuated indices of left ventricular dilation and infarct expansion. We speculated that the attenuation in apoptosis and inflammatory infiltration could contribute to reduced chronic infarct scar size in the MRL. We concluded that attenuated apoptosis and inflammatory infiltration could be the source of the MRL's survival and healing phenotypes, but may be derived in part from its shared genetic background with the LG/J.

This work contributes to our understanding of the components of the acute post-MI healing response that affect both early survival and long-term healing, and illustrates the utility of genome-wide analysis to gain mechanistic insight into these traits.

Analysis of gene expression using targeted or genome-wide microarrays has become an important tool in cardiovascular research [178]. Profiling thousands to tens of thousands of genes allows an unbiased view of the transcriptional signature unique to a particular disease state. But because hundreds of genes can meet the criteria for significant expression, methods to divide them into groups based on function and/or expression pattern are quite useful. Functional analysis of gene expression data using MAPPFinder [162] and the Gene Ontology (www.geneontology.org) has been used to characterize pressure overload-induced hypertrophy [179] and doxorubicin-induced cardiomyopathy [180]. Hierarchical clustering has been used to investigate gene expression patterns in diseases such as heart failure [181] and ischemic and non-ischemic cardiomyopathy [182]. Here we have combined these methods in a manner similar to Zambon and colleagues [183] to first group genes according to their expression patterns, and then to assign functional significance to these groups by annotating them with Gene Ontology terms, using MAPPFinder.

The results of this analysis and subsequent tissue-level assays have contributed to existing evidence that targeting specific components of the acute post-MI healing response may influence survival and remodeling, as discussed in Chapter 1. Post-MI healing begins with myocyte necrosis, an inflammatory response, apoptosis, and the degradation of existing extracellular matrix. Deposition of granulation tissue as a provisional matrix accompanies the resolution of the inflammatory response. Collagen deposition accompanies apoptosis of the granulation tissue, and continues along with myocyte hypertrophy and global remodeling of the left ventricle as the infarct scar

matures. In agreement with previous reports [20,26,54,58-60,72,169,171,172,184], we have shown that reductions in acute apoptosis and inflammatory infiltration (in MRL hearts) are associated with both increased early survival and attenuated chronic remodeling. In conjunction with our microarray analysis, these results could be used in the future to therapeutically target the genes or pathways responsible for attenuated apoptosis and inflammation in this model of post-MI healing.

4.3 Limitations and Future Directions

There are several limitations in the design of these studies, some of which could be addressed in future work. First, in order to perform tissue-level assays at different time points, it is necessary to sacrifice a cohort of animals at each time point. This means that quantities measured over time are measured in different animals at each endpoint. Ideally, we would like to know how a quantity such as the expression of certain mRNA transcripts varies over time in the same animals, but it is impossible to directly measure mRNA expression without sacrificing the animal. The same limitation applies to infarct size. Techniques such as delayed contrast-enhanced magnetic resonance imaging do not provide high enough resolution to precisely measure infarct size in mice, so the time course of infarct size must be measured in a different cohort of animals at each endpoint. We have attempted to ameliorate this problem by measuring initial infarct size after 1 day to show that, on average, animals receive the same size infarcts.

In our study of post-MI healing in biglycan-null mice, we relied on tracking surface markers on the infarct *in vivo* to measure the strain experienced by the infarct over the cardiac cycle. This assumed that the 3 points chosen for analysis remained in the plane of video capture during that time, and that the only movement relative to each other was due to stretch or compression in that plane. We attempted to stabilize the hearts while recording these data to minimize the effect of out-of-plane motion while the hearts were beating, but it is possible that there were artifacts added to the data due to the heart rolling relative to the video capture plane. A more accurate measurement of infarct scar stiffness might be gained by isolating the hearts and subjecting them to an inflation pressure [148], thereby avoiding movement due to beating. The study could also be improved by lengthening the post-MI time period so that the mice have the opportunity to descend into heart failure. This would allow the testing of the hypothesis that biglycan is protective in the setting of failure. Functional measurements such as ejection fraction and LV end-systolic and end-diastolic diameters would also be useful to determine if LV pump function is improved in biglycan-null mice.

In our study of survival and healing in the MRL, we did not measure the gelatinolytic activity of MMP-2 and MMP-9, enzymes which are widely believed to play a causal role in ventricular rupture. These enzymes must undergo post-translational processing before becoming active, so measurement of mRNA levels is not sufficient. Possible future results of reduced MMP-9 activity in the first 2-4 days after MI in the MRL would provide additional support to our conclusion that increased survival in the MRL is due to mechanisms that prevent rupture. Increasing the number of LG/J animals

would enable a more accurate picture of its rupture rate, and determine if it is significantly different from either the C57 or the MRL. MMP activity could also be investigated in LG/J animals. These additional studies at acute endpoints would enable a better characterization of how much the LG/J's genetic background contributes to the MRL's increased survival.

Finally, future studies could investigate the source of the BrdU-positive cells in the C57 and MRL myocardium. This could involve additional immunolabeling for a marker of cardiac muscle, as well as markers for cardiac progenitor cells as discussed earlier. The results of this experiment would provide new information on whether adult myocytes are induced to divide, or if any BrdU-positive myocytes could have arisen from a known population of resident progenitor cells.

References

1. National Center for Health Statistics: Deaths/Mortality.

2. Anversa P, Nadal-Ginard B. Myocyte renewal and ventricular remodelling. *Nature* 2002;415(6868):240-243.

3. Beltrami AP, Urbanek K, Kajstura J, Yan S-M, Finato N, Bussani R, et al. Evidence That Human Cardiac Myocytes Divide after Myocardial Infarction. *N Engl J Med* 2001;344(23):1750-1757.

4. Pfeffer MA, Braunwald E. Ventricular Remodeling After Myocardial Infarction. *Circulation* 1990;81(4):1161-1172.

5. Pfeffer MA, Pfeffer JM, Fishbein MC, Fletcher PJ, Spadaro J, Kloner RA, et al. Myocardial infarct size and ventricular function in rats. *Circ Res* 1979;44(4):503-512.

6. van den Borne SWM, Cleutjens JPM, Hanemaaijer R, Creemers EE, Smits JFM, Daemen MJAP, et al. Increased matrix metalloproteinase-8 and -9 activity in patients with infarct rupture after myocardial infarction. *Cardiovascular Pathology* 2009;18(1):37-43.

7. Pfeffer JM, Pfeffer MA, Fletcher PJ, Braunwald E. Progressive ventricular remodeling in rat with myocardial infarction. *Am J Physiol Heart Circ Physiol* 1991;260(5):H1406-1414.

8. Tao Z-Y, Cavasin MA, Yang F, Liu Y-H, Yang X-P. Temporal changes in matrix metalloproteinase expression and inflammatory response associated with cardiac rupture after myocardial infarction in mice. *Life Sciences* 2004;74(12):1561-1572.

9. Frangogiannis NG. Targeting the inflammatory response in healing myocardial infarcts. *Current Medicinal Chemistry* 2006;13(16):1877-1893.

10. Nian M, Lee P, Khaper N, Liu P. Inflammatory Cytokines and Postmyocardial Infarction Remodeling. *Circ Res* 2004;94(12):1543-1553.

11. Witte MB, Barbul A. General Principles of Wound Healing. *Surgical Clinics of North America* 1997;77(3):509-528.

12. Yang F, Liu Y-H, Yang X-P, Xu J, Kapke A, Carretero OA. Myocardial Infarction and Cardiac Remodelling in Mice. *Experimental Physiology* 2002;87(5):547-555.

13. Deten A, Volz HC, Briest W, Zimmer H-G. Cardiac cytokine expression is upregulated in the acute phase after myocardial infarction. Experimental studies in rats. *Cardiovascular Research* 2002;55(2):329-340.

14. Dobaczewski M, Bujak M, Zymek P, Ren G, Entman M, Frangogiannis N. Extracellular matrix remodeling in canine and mouse myocardial infarcts. *Cell and Tissue Research* 2006;324(3):475-488.

15. Entman ML, Michael L, Rossen RD, Dreyer WJ, Anderson DC, Taylor AA, et al. Inflammation in the course of early myocardial ischemia. *FASEB J.* 1991;5(11):2529-2537.

16. Frangogiannis NG, Smith CW, Entman ML. The inflammatory response in myocardial infarction. *Cardiovascular Research* 2002;53(1):31-47.

17. Kurrelmeyer KM, Michael LH, Baumgarten G, Taffet GE, Peschon JJ, Sivasubramanian N, et al. Endogenous tumor necrosis factor protects the adult cardiac myocyte against ischemic-induced apoptosis in a murine model of acute myocardial infarction. *PNAS* 2000;97(10):5456-5461.

18. MacEwan DJ. TNF ligands and receptors — a matter of life and death. *Br J Pharmacol* 2002;135(4):855-875.

19. Irwin MW, Mak S, Mann DL, Qu R, Penninger JM, Yan A, et al. Tissue Expression and Immunolocalization of Tumor Necrosis Factor-α in Postinfarction Dysfunctional Myocardium. *Circulation* 1999;99(11):1492-1498.

20. Heymans S, Luttun A, Nuyens D, Theilmeier G, Creemers E, Moons L, et al. Inhibition of plasminogen activators or matrix metalloproteinases prevents cardiac rupture but impairs therapeutic angiogenesis and causes cardiac failure. 1999;5(10):1135-1142.

21. Sun M, Dawood F, Wen W-H, Chen M, Dixon I, Kirshenbaum LA, et al. Excessive Tumor Necrosis Factor Activation After Infarction Contributes to Susceptibility of Myocardial Rupture and Left Ventricular Dysfunction. *Circulation* 2004;110(20):3221-3228.

22. Bradham WS, Bozkurt B, Gunasinghe H, Mann D, Spinale FG. Tumor necrosis factor-alpha and myocardial remodeling in progression of heart failure: a current perspective. *Cardiovasc Res* 2002;53(4):822-830.

23. Heinrich PC, Behrmann I, Haan S, Hermanns HM, MÃ¼ller-Newen G, Schaper F. Principles of interleukin (IL)-6-type cytokine signalling and its regulation. *Biochem. J.* 2003;374(1):1-20.

24. Banerjee I, Fuseler JW, Intwala AR, Baudino TA. IL-6 loss causes ventricular dysfunction, fibrosis, reduced capillary density, and dramatically alters the cell populations of the developing and adult heart. *Am J Physiol Heart Circ Physiol* 2009;296(5):H1694-1704.

25. Fuchs M, Hilfiker A, Kaminski K, Hilfiker-Kleiner D, Guener Z, Klein G, et al. Role of interleukin-6 for left ventricular remodeling and survival after experimental myocardial infarction. *FASEB J.* 2003:03-0331fje.

26. Moon C, Krawczyk M, Ahn D, Ahmet I, Paik D, Lakatta EG, et al. Erythropoietin reduces myocardial infarction and left ventricular functional decline after coronary artery ligation in rats. *PNAS* 2003;100(20):11612-11617.

27. Gao X-M, Xu Q, Kiriazis H, Dart AM, Du X-J. Mouse model of post-infarct ventricular rupture: time course, strain- and gender-dependency, tensile strength, and histopathology. *Cardiovasc Res* 2005;65(2):469-477.

28. Lindsey M, Wedin K, Brown MD, Keller C, Evans AJ, Smolen J, et al. Matrix-Dependent Mechanism of Neutrophil-Mediated Release and Activation of Matrix Metalloproteinase 9 in Myocardial Ischemia/Reperfusion. *Circulation* 2001;103(17):2181-2187.

29. Chen J, Tung C-H, Allport JR, Chen S, Weissleder R, Huang PL. Near-Infrared Fluorescent Imaging of Matrix Metalloproteinase Activity After Myocardial Infarction. *Circulation* 2005;111(14):1800-1805.

30. Vanhoutte D, Schellings M, Pinto Y, Heymans S. Relevance of matrix metalloproteinases and their inhibitors after myocardial infarction: A temporal and spatial window. *Cardiovascular Research* 2006;69(3):604-613.

31. Spinale FG. Matrix Metalloproteinases: Regulation and Dysregulation in the Failing Heart. *Circ Res* 2002;90(5):520-530.

32. Ducharme A, Frantz S, Aikawa M, Rabkin E, Lindsey M, Rohde LE, et al. Targeted deletion of matrix metalloproteinase-9 attenuates left ventricular enlargement and collagen accumulation after experimental myocardial infarction. *J. Clin. Invest.* 2000;106(1):55-62.

33. Cleutjens JPM, Kandala JC, Guarda E, Guntaka RV, Weber KT. Regulation of collagen degradation in the rat myocardium after infarction. *Journal of Molecular and Cellular Cardiology* 1995;27(6):1281-1292.

34. Creemers EEJM, Davis JN, Parkhurst AM, Leenders P, Dowdy KB, Hapke E, et al. Deficiency of TIMP-1 exacerbates LV remodeling after myocardial infarction in mice. *Am J Physiol Heart Circ Physiol* 2003;284(1):H364-371.

35. Heymans S, Lupu F, Terclavers S, Vanwetswinkel B, Herbert J-M, Baker A, et al. Loss or Inhibition of uPA or MMP-9 Attenuates LV Remodeling and Dysfunction after Acute Pressure Overload in Mice. *Am J Pathol* 2005;166(1):15-25.

36. Webb CS, Bonnema DD, Ahmed SH, Leonardi AH, McClure CD, Clark LL, et al. Specific Temporal Profile of Matrix Metalloproteinase Release Occurs in Patients After Myocardial Infarction: Relation to Left Ventricular Remodeling. *Circulation* 2006;114(10):1020-1027.

37. Lindsey ML, Escobar GP, Dobrucki LW, Goshorn DK, Bouges S, Mingoia JT, et al. Matrix metalloproteinase-9 gene deletion facilitates angiogenesis after myocardial infarction. *Am J Physiol Heart Circ Physiol* 2006;290(1):H232-239.

38. Hudson MP, Armstrong PW, Ruzyllo W, Brum J, Cusmano L, Krzeski P, et al. Effects of Selective Matrix Metalloproteinase Inhibitor (PG-116800) to Prevent Ventricular Remodeling After Myocardial Infarction: Results of the PREMIER (Prevention of Myocardial Infarction Early Remodeling) Trial. *Journal of the American College of Cardiology* 2006;48(1):15-20.

39. Hayashidani S, Tsutsui H, Ikeuchi M, Shiomi T, Matsusaka H, Kubota T, et al. Targeted deletion of MMP-2 attenuates early LV rupture and late remodeling after experimental myocardial infarction. *Am J Physiol Heart Circ Physiol* 2003;285(3):H1229-1235.

40. Matsumura S-i. Targeted deletion or pharmacological inhibition of MMP-2 prevents cardiac rupture after myocardial infarction in mice. *The Journal of Clinical Investigation* 2005;115(3):599-609.

41. Carmeliet P, Moons L, Lijnen R, Baes M, Lemaitre V, Tipping P, et al. Urokinase-generated plasmin activates matrix metalloproteinases during aneurysm formation. *Nat Genet* 1997;17(4):439-444.

42. Hutchins G, Bulkley B. Infarct expansion versus extension: two different complications of acute myocardial infarction. *Am J Cardiol* 1978;41(7):1127-1132.

43. Weisman HF, Bush DE, Mannisi JA, Weisfeldt ML, Healy B. Cellular mechanisms of myocardial infarct expansion. *Circulation* 1988;78(1):186-201.

44. Creemers EEJM, Cleutjens JPM, Smits JFM, Daemen MJAP. Matrix Metalloproteinase Inhibition After Myocardial Infarction: A New Approach to Prevent Heart Failure? *Circ Res* 2001;89(3):201-210.

45. Kaikita K, Hayasaki T, Okuma T, Kuziel WA, Ogawa H, Takeya M. Targeted Deletion of CC Chemokine Receptor 2 Attenuates Left Ventricular Remodeling after Experimental Myocardial Infarction. *Am J Pathol* 2004;165(2):439-447.

46. Peterson JT, Li H, Dillon L, Bryant JW. Evolution of matrix metalloprotease and tissue inhibitor expression during heart failure progression in the infarcted rat. *Cardiovasc Res* 2000;46(2):307-315.

47. Takemura G, Fujiwara H. Role of apoptosis in remodeling after myocardial infarction. *Pharmacology & Therapeutics* 2004;104(1):1-16.

48. Bialik S, Geenen DL, Sasson IE, Cheng R, Horner JW, Evans SM, et al. Myocyte Apoptosis During Acute Myocardial Infarction in the Mouse Localizes to Hypoxic Regions but Occurs Independently of p53. *J. Clin. Invest.* 1997;100(6):1363-1372.

49. Xu T, Bianco P, Fisher LW, Longenecker G, Smith E, Goldstein S, et al. Targeted disruption of the biglycan gene leads to an osteoporosis-like phenotype in mice. *Nat Genet* 1998;20(1):78-82.

50. Gill C, Mestril R, Samali A. Losing heart: the role of apoptosis in heart disease--a novel therapeutic target? *FASEB J.* 2002;16(2):135-146.

51. Jeremias I, Kupatt C, Martin-Villalba A, Habazettl H, Schenkel J, Boekstegers P, et al. Involvement of CD95/Apo1/Fas in Cell Death After Myocardial Ischemia. *Circulation* 2000;102(8):915-920.

52. Lee P, Sata M, Lefer DJ, Factor SM, Walsh K, Kitsis RN. Fas pathway is a critical mediator of cardiac myocyte death and MI during ischemia-reperfusion in vivo. *Am J Physiol Heart Circ Physiol* 2003;284(2):H456-463.

53. Wollert KC, Heineke J, Westermann J, Ludde M, Fiedler B, Zierhut W, et al. The Cardiac Fas (APO-1/CD95) Receptor/Fas Ligand System : Relation to Diastolic Wall Stress in Volume-Overload Hypertrophy In Vivo and Activation of the Transcription Factor AP-1 in Cardiac Myocytes. *Circulation* 2000;101(10):1172-1178.

54. Liehn EA, Merx MW, Postea O, Becher S, Djalali-Talab Y, Shagdarsuren E, et al. Ccr1 deficiency reduces inflammatory remodelling and preserves left ventricular function after myocardial infarction. *Journal of Cellular and Molecular Medicine* 2008;12(2):496-506.

55. Kajstura J, Cheng W, Reiss K, Clark WA, Sonnenblick E, Krajewski S, et al. Apoptotic and necrotic myocyte cell deaths are independent contributing variables of infarct size in rats. *Lab Invest* 1996;74(1):86-107.

56. Cheng W, Kajstura J, Nitahara JA, Li B, Reiss K, Liu Y, et al. Programmed Myocyte Cell Death Affects the Viable Myocardium after Infarction in Rats. *Experimental Cell Research* 1996;226(2):316-327.

57. Kocher AA, Schuster MD, Szabolcs MJ, Takuma S, Burkhoff D, Wang J, et al. Neovascularization of ischemic myocardium by human bone-marrow-derived angioblasts prevents cardiomyocyte apoptosis, reduces remodeling and improves cardiac function. *Nat Med* 2001;7(4):430-436.

58. Erlich JH, Boyle EM, Labriola J, Kovacich JC, Santucci RA, Fearns C, et al. Inhibition of the Tissue Factor-Thrombin Pathway Limits Infarct Size after Myocardial Ischemia-Reperfusion Injury by Reducing Inflammation. *Am J Pathol* 2000;157(6):1849-1862.

59. Wu Y, Tu X, Lin G, Xia H, Huang H, Wan J, et al. Emodin-mediated protection from acute myocardial infarction via inhibition of inflammation and apoptosis in local ischemic myocardium. *Life Sciences* 2007;81(17-18):1332-1338.

60. Yao Y-Y, Yin H, Shen B, Chao L, Chao J. Tissue kallikrein infusion prevents cardiomyocyte apoptosis, inflammation and ventricular remodeling after myocardial infarction. *Regulatory Peptides* 2007;140(1-2):12-20.

61. Vinten-Johansen J. Involvement of neutrophils in the pathogenesis of lethal myocardial reperfusion injury. *Cardiovasc Res* 2004;61(3):481-497.

62. Jugdutt BI, Basualdo C. Myocardial infarct expansion during indomethacin or ibuprofen therapy for symptomatic post infarction pericarditis. Influence of other pharmacologic agents during early remodelling. *Can J Cardiol* 1989;5(4):211-221.

63. Roberts R, DeMello V, Sobel B. Deleterious effects of methylprednisolone in patients with myocardial infarction. *Circulation* 1976;53(3 Suppl):I204-6.

64. Baran KW, Nguyen M, McKendall GR, Lambrew CT, Dykstra G, Palmeri ST, et al. Double-Blind, Randomized Trial of an Anti-CD18 Antibody in Conjunction With Recombinant Tissue Plasminogen Activator for Acute Myocardial Infarction: Limitation of Myocardial Infarction Following Thrombolysis in Acute Myocardial Infarction (LIMIT AMI) Study. *Circulation* 2001;104(23):2778-2783.

65. Faxon DP, Gibbons RJ, Chronos NAF, Gurbel PA, Sheehan F. The effect of blockade of the CD11/CD18 integrin receptor on infarct size in patients with acute myocardial infarction treated with direct angioplasty: the results of the HALT-MI study. *Journal of the American College of Cardiology* 2002;40(7):1199-1204.

66. Creemers E, Cleutjens J, Smits J, Heymans S, Moons L, Collen D, et al. Disruption of the Plasminogen Gene in Mice Abolishes Wound Healing after Myocardial Infarction. *Am J Pathol* 2000;156(6):1865-1873.

67. Lindsey ML, Gannon J, Aikawa M, Schoen FJ, Rabkin E, Lopresti-Morrow L, et al. Selective Matrix Metalloproteinase Inhibition Reduces Left Ventricular Remodeling but Does Not Inhibit Angiogenesis After Myocardial Infarction. *Circulation* 2002;105(6):753-758.

68. Yarbrough WM, Mukherjee R, Escobar GP, Mingoia JT, Sample JA, Hendrick JW, et al. Selective Targeting and Timing of Matrix Metalloproteinase Inhibition in Post-Myocardial Infarction Remodeling. *Circulation* 2003;108(14):1753-1759.

69. Takayama S, Reed JC, Homma S. Heat-shock proteins as regulators of apoptosis. *Oncogene* 2003;22(56):9041-9047.

70. Hutter JJ, Mestril R, Tam EKW, Sievers RE, Dillmann WH, Wolfe CL. Overexpression of Heat Shock Protein 72 in Transgenic Mice Decreases Infarct Size In Vivo. *Circulation* 1996;94(6):1408-1411.

71. Zhang C, Xu Z, He X-R, Michael LH, Patterson C. CHIP, a cochaperone/ubiquitin ligase that regulates protein quality control, is required for maximal cardioprotection after myocardial infarction in mice. *Am J Physiol Heart Circ Physiol* 2005;288(6):H2836-2842.

72. Calvillo L, Latini R, Kajstura J, Leri A, Anversa P, Ghezzi P, et al. Recombinant human erythropoietin protects the myocardium from ischemia-reperfusion injury and promotes beneficial remodeling. *PNAS* 2003;100(8):4802-4806.

73. Namiuchi S, Kagaya Y, Ohta J, Shiba N, Sugi M, Oikawa M, et al. High Serum Erythropoietin Level Is Associated With Smaller Infarct Size in Patients With Acute Myocardial Infarction Who Undergo Successful Primary Percutaneous Coronary Intervention. *Journal of the American College of Cardiology* 2005;45(9):1406-1412.

74. Lipšic E, van der Meer P, Voors A, Westenbrink B, van den Heuvel A, de Boer H, et al. A Single Bolus of a Long-acting Erythropoietin Analogue Darbepoetin Alfa in Patients with Acute Myocardial Infarction: A Randomized Feasibility and Safety Study. *Cardiovascular Drugs and Therapy* 2006;20(2):135-141.

75. Liem A, van de Woestijne AP, Bruijns E, Roeters van Lennep HWO, de Boo JAJ, van Halteren HK, et al. Effect of EPO administration on myocardial infarct size in patients with non-STE acute coronary syndromes; results from a pilot study. *International Journal of Cardiology* 2009;131(2):285-287.

76. Andreotti F, Agati L, Conti E, Santucci E, Rio T, Tarantino F, et al. Update on phase II studies of erythropoietin in acute myocardial infarction. Rationale and design of Exogenous erythroPoietin in Acute Myocardial Infarction: New Outlook aNd Dose Association Study (EPAMINONDAS). *Journal of Thrombosis and Thrombolysis* 2009:Published online before print.

77. Virag JI, Murry CE. Myofibroblast and Endothelial Cell Proliferation during Murine Myocardial Infarct Repair. *Am J Pathol* 2003;163(6):2433-2440.

78. Krishnamurthy P, Rajasingh J, Lambers E, Qin G, Losordo DW, Kishore R. IL-10 Inhibits Inflammation and Attenuates Left Ventricular Remodeling After Myocardial Infarction via Activation of STAT3 and Suppression of HuR. *Circ Res* 2009;104(2):e9-18.

79. Frangogiannis NG, Mendoza LH, Lindsey ML, Ballantyne CM, Michael LH, Smith CW, et al. IL-10 Is Induced in the Reperfused Myocardium and May Modulate the Reaction to Injury. *J Immunol* 2000;165(5):2798-2808.

80. Huynh M-LN, Fadok VA, Henson PM. Phosphatidylserine-dependent ingestion of apoptotic cells promotes TGF-β1 secretion and the resolution of inflammation. *J Clin Invest* 2002;109(1):41-50.

81. Ikeuchi M, Tsutsui H, Shiomi T, Matsusaka H, Matsushima S, Wen J, et al. Inhibition of TGF-β signaling exacerbates early cardiac dysfunction but prevents late remodeling after infarction. *Cardiovascular Research* 2004;64(3):526-535.

82. Ruiz-Ortega M, Rodriguez-Vita J, Sanchez-Lopez E, Carvajal G, Egido J. TGF-β signaling in vascular fibrosis. *Cardiovasc Res* 2007;74(2):196-206.

83. Schellings MWM, Pinto YM, Heymans S. Matricellular proteins in the heart: possible role during stress and remodeling. *Cardiovasc Res* 2004;64(1):24-31.

84. Takemura G, Ohno M, Hayakawa Y, Misao J, Kanoh M, Ohno A, et al. Role of Apoptosis in the Disappearance of Infiltrated and Proliferated Interstitial Cells After Myocardial Infarction. *Circ Res* 1998;82(11):1130-1138.

85. Jugdutt BI. Ventricular Remodeling After Infarction and the Extracellular Collagen Matrix: When Is Enough Enough? *Circulation* 2003;108(11):1395-1403.

86. Mann DL. Inflammatory Mediators and the Failing Heart: Past, Present, and the Foreseeable Future. *Circ Res* 2002;91(11):988-998.

87. Akyürek Ö, Akyürek N, Sayin T, Dinçer I, Berkalp B, Akyol G, et al. Association between the severity of heart failure and the susceptibility of myocytes to apoptosis in patients with idiopathic dilated cardiomyopathy. *International Journal of Cardiology* 2001;80(1):29-36.

88. Neil BR, Aldwyn JH, Brendan M, Andrew M, Rod T, Martin S, et al. Myocyte loss in chronic heart failure. *The Journal of Pathology* 1999;188(2):213-219.

89. Ono K, Matsumori A, Shioi T, Furukawa Y, Sasayama S. Cytokine Gene Expression After Myocardial Infarction in Rat Hearts : Possible Implication in Left Ventricular Remodeling. *Circulation* 1998;98(2):149-156.

90. Bryant D, Becker L, Richardson J, Shelton J, Franco F, Peshock R, et al. Cardiac Failure in Transgenic Mice With Myocardial Expression of Tumor Necrosis Factor-{alpha}. *Circulation* 1998;97(14):1375-1381.

91. Sivasubramanian N, Coker ML, Kurrelmeyer KM, MacLellan WR, DeMayo FJ, Spinale FG, et al. Left Ventricular Remodeling in Transgenic Mice With Cardiac Restricted Overexpression of Tumor Necrosis Factor. *Circulation* 2001;104(7):826-831.

92. Sun Y, Weber KT. Infarct scar: a dynamic tissue. *Cardiovasc Res* 2000;46(2):250-256.

93. Eghbali M, Tomek R, Woods C, Bhambi B. Cardiac fibroblasts are predisposed to convert into myocyte phenotype: specific effect of transforming growth factor beta. *Proceedings of the National Academy of Sciences of the United States of America* 1991;88(3):795-799.

94. Jugdutt BI. Remodeling of the Myocardium and Potential Targets in the Collagen Degradation and Synthesis Pathways. *Current Drug Targets -Cardiovascular & Haematological Disorders* 2003;3:1-30.

95. Holmes JW, Borg TK, Covell JW. Structure and mechanics of healing myocardial infarcts. *Annual Review of Biomedical Engineering* 2005;7(1):223-253.

96. Pfeffer MA. Left Ventricular Remodeling After Acute Myocardial Infarction. *Annual Review of Medicine* 1995;46(1):455-466.

97. Anversa P, Beghi C, Kikkawa Y, Olivetti G. Myocardial infarction in rats. Infarct size, myocyte hypertrophy, and capillary growth. *Circ Res* 1986;58(1):26-37.

98. Alberts B, Johnson A, Lewis J, Raff M, Roberts K, Walter P. *Molecular Biology of the Cell*. 4 ed: Garland, 2002.

99. Ameye L, Aria D, Jepsen K, Oldberg A, Xu T, Young MF. Abnormal collagen fibrils in tendons of biglycan/fibromodulin-deficient mice lead to gait impairment, ectopic ossification, and osteoarthritis. *FASEB J.* 2002;16(7):673-80.

100. Goldberg M, Rapoport O, Septier D, Palmier K, Hall R, Embery G, et al. Proteoglycans in predentin: the last 15 micrometers before mineralization. *Connect. Tissue. Res.* 2003;44(Suppl 1):184-188.

101. San Martin S, Soto-Suazo M, Ferreira de Oliveira S, Aplin JD, Abrahamsohn P, Zorn TMT. Small Leucine-rich proteoglycans (SLRPs) in uterine tissues during pregnancy in mice. *Reproduction* 2003;125(4):585-595.

102. Hocking AM, Shinomura T, McQuillan DJ. Leucine-rich repeat glycoproteins of the extracellular matrix. *Matrix Biol* 1998;17:1-19.

103. Schönherr E, Witsch-Prehm P, Harrach B, Robenek H, Rauterberg J, Kresse H. Interaction of Biglycan with Type I Collagen. *J. Biol. Chem.* 1995;270(6):2776-2783.

104. Vogel KG, Trotter JA. The effect of proteoglycans on the morphology of collagen fibrils formed in vitro. *Coll Relat Res* 1987;7(2):105-114.

105. Chen XD, Shi S, Xu T, Robey PG, Young MF. Age-Related Osteoporosis in Biglycan-Deficient Mice is Related to Defects in Bone Marrow Stromal Cells. *J. Bone Miner. Res.* 2002;17:331-340.

106. Heegaard AM, Corsi A, Danielsen CC, Nielsen KL, Jorgensen HL, Riminucci M, et al. Biglycan deficiency causes spontaneous aortic dissection and rupture in mice. *Circulation* 2007;115(21):2731-2738.

107. Danielson KG, Baribault H, Holmes DF, Graham H, Kadler KE, Iozzo RV. Targeted Disruption of Decorin Leads to Abnormal Collagen Fibril Morphology and Skin Fragility. *J. Cell Biol.* 1997;136(3):729-743.

108. Campbell P, Hunt D, Jones Y, Harwood FL, Amiel D, Omens JH, et al. Effects of biglycan deficiency on myocardial infarct structure and mechanics. *Mol Cell Biomech* 2008;5(1):27-35.

109. Brockes JP, Kumar A. Plasticity and reprogramming of differentiated cells in amphibian regeneration. *Nat Rev Mol Cell Biol* 2002;3(8):566-574.

110. Poss KD, Wilson LG, Keating MT. Heart Regeneration in Zebrafish. *Science* 2002;298(5601):2188-2190.

111. Blewett CJ, Cilley RE, Ehrlich HP, Blackburn JH, II, Dillon PW, Krummel TM. Regenerative healing of incisional wounds in midgestational murine hearts in organ culture. *J Thorac Cardiovasc Surg* 1997;113(5):880-885.

112. Linke A, Muller P, Nurzynska D, Casarsa C, Torella D, Nascimbene A, et al. Stem cells in the dog heart are self-renewing, clonogenic, and multipotent and

regenerate infarcted myocardium, improving cardiac function. *PNAS* 2005;102(25):8966-8971.

113. Martin CM, Meeson AP, Robertson SM, Hawke TJ, Richardson JA, Bates S, et al. Persistent expression of the ATP-binding cassette transporter, Abcg2, identifies cardiac SP cells in the developing and adult heart. *Developmental Biology* 2004;265(1):262-275.

114. Oh H, Bradfute SB, Gallardo TD, Nakamura T, Gaussin V, Mishina Y, et al. Cardiac progenitor cells from adult myocardium: Homing, differentiation, and fusion after infarction. *PNAS* 2003;100(21):12313-12318.

115. Bearzi C, Rota M, Hosoda T, Tillmanns J, Nascimbene A, De Angelis A, et al. Human cardiac stem cells. *Proceedings of the National Academy of Sciences* 2007;104(35):14068-14073.

116. Pfister O, Mouquet F, Jain M, Summer R, Helmes M, Fine A, et al. CD31- but Not CD31+ Cardiac Side Population Cells Exhibit Functional Cardiomyogenic Differentiation. *Circ Res* 2005;97(1):52-61.

117. Matsuura K, Nagai T, Nishigaki N, Oyama T, Nishi J, Wada H, et al. Adult Cardiac Sca-1-positive Cells Differentiate into Beating Cardiomyocytes. *J. Biol. Chem.* 2004;279(12):11384-11391.

118. Rota M, Padin-Iruegas ME, Misao Y, De Angelis A, Maestroni S, Ferreira-Martins J, et al. Local Activation or Implantation of Cardiac Progenitor Cells Rescues Scarred Infarcted Myocardium Improving Cardiac Function. *Circ Res* 2008;103(1):107-116.

119. Beltrami AP, Barlucchi L, Torella D, Baker M, Limana F, Chimenti S, et al. Adult Cardiac Stem Cells Are Multipotent and Support Myocardial Regeneration. *Cell* 2003;114(6):763-776.

120. Urbanek K, Rota M, Cascapera S, Bearzi C, Nascimbene A, De Angelis A, et al. Cardiac Stem Cells Possess Growth Factor-Receptor Systems That After Activation Regenerate the Infarcted Myocardium, Improving Ventricular Function and Long-Term Survival. *Circ Res* 2005;97(7):663-673.

121. Colwell AS, Longaker MT, Lorenz HP. Mammalian Fetal Organ Regeneration. *Advances in Biochemical Engineering/Biotechnology* 2005;93:83-100.

122. Clark LD, Clark RK, Heber-Katz E. A New Murine Model for Mammalian Wound Repair and Regeneration. *Clinical Immunology and Immunopathology* 1998;88(1):35-45.

123. Leferovich JM, Bedelbaeva K, Samulewicz S, Zhang X-M, Zwas D, Lankford EB, et al. Heart regeneration in adult MRL mice. *PNAS* 2001;98(17):9830-9835.

124. Heber-Katz E, Leferovich J, Bedelbaeva K, Gourevitch D, Clark L. The scarless heart and the MRL mouse. *Phil. Trans. R. Soc. Lond. B* 2004;359(1445):785-793.

125. Oh Y-S, Thomson LEJ, Fishbein MC, Berman DS, Sharifi B, Chen P-S. Scar formation after ischemic myocardial injury in MRL mice. *Cardiovascular Pathology* 2004;13(4):203-206.

126. Abdullah I, Lepore JJ, Epstein JA, Parmacek MS, Gruber PJ. MRL mice fail to heal the heart in response to ischemia-reperfusion injury. *Wound Repair and Regeneration* 2005;13(2):205-208.

127. Cimini M, Fazel S, Fujii H, Zhou S, Tang G, Weisel RD, et al. The MRL mouse heart does not recover ventricular function after a myocardial infarction. *Cardiovascular Pathology* 2008;17(1):32-39.

128. Grisel P, Meinhardt A, Lehr H-A, Kappenberger L, Barrandon Y, Vassalli G. The MRL mouse repairs both cryogenic and ischemic myocardial infarcts with scar. *Cardiovascular Pathology* 2008;17(1):14-22.

129. Robey TE, Murry CE. Absence of regeneration in the MRL/MpJ mouse heart following infarction or cryoinjury. *Cardiovascular Pathology* 2008;17(1):6-13.

130. Naseem RH, Meeson AP, Michael DiMaio J, White MD, Kallhoff J, Humphries C, et al. Reparative myocardial mechanisms in adult C57BL/6 and MRL mice following injury. *Physiol. Genomics* 2007;30(1):44-52.

131. Borg TK, Caulfield JB. The collagen matrix of the heart. *Fed Proc.* 1981;40(7):2037-41.

132. Sussman MA, McCulloch A, Borg TK. Dance band on the Titanic: biomechanical signaling in cardiac hypertrophy. *Circ. Res.* 2002;91(10):888-898.

133. Kawaguchi H, Kitabatake A. Renin-angiotensin system in failing heart. *J. Mol. Cell. Cardiol.* 1995;27(1):201-209.

134. Ezura Y, Chakravarti S, Oldberg A, Chervoneva I, Birk DE. Differential expression of lumican and fibromodulin regulate collagen fibrillogenesis in developing mouse tendons. *J. Cell. Biol.* 2000;151(4):779-88.

135. Kuc IM, Scott PG. Increased diameters of collagen fibrils precipitated in vitro in the presence of decorin from various connective tissues. *Connect. Tissue. Res.* 1997;36(4):287-296.

136. Iozzo RV, Murdoch AD. Proteoglycans of the extracellular environment: clues from the gene and protein side offer novel perspectives in molecular diversity of function. *FASEB J.* 1996;10:598-614.

137. Iozzo RV. Matrix proteoglycans: from molecular design to cellular function. *Annu. Rev. Biochem.* 1998;67:609-52.

138. Hildebrand A, Romarís M, Rasmussen LM, Heinegård D, Twardzik DR, Border WA, et al. Interaction of the small interstitial proteoglycans biglycan, decorin and fibromodulin with transforming growth factor beta. *Biochem. J.* 1994;302(2):527-34.

139. Yamamoto K, Kusachi S, Ninomiya Y, Murakami M, Doi M, Takeda K, et al. Increase in the Expression of Biglycan mRNA Expression Co-localized Closely with that of Type I Collagen mRNA in the Infarct Zone After Experimentally-Induced Myocardial Infarction in Rats. *J. Mol. Cell. Cardiol.* 1998;30:1749-1756.

140. Lie JT, Pairolero PC, Holley KE, Titus JL. Macroscopic enzyme-mapping verification of large, homogeneous, experimental myocardial infarcts of predictable size and location in dogs. *J. Thorac. Cardiovasc. Surg.* 1975;69(4):599-605.

141. Ytrehus K, Liu Y, Tsuchida A, Miura T, Liu GS, Yang X, et al. Rat and rabbit heart infarction: effects of anesthesia, perfusate, risk zone, and method of infarct sizing. *Am. J. Physiol.* 1994;267(6 Pt 2):H2383-90.

142. MacKenna DA, Omens JH, McCulloch AD, Covell JW. Contribution of collagen matrix to passive left ventricular mechanics in isolated rat hearts. *Am. J. Physiol.* 1994;266(3 Pt 2):H1007-H1018.

143. Woessner JF. The determination of hydroxyproline in tissue and protein samples containing small proportions of this imino acid. *Archives of Biochemistry and Biophysics* 1961;93(2):440-447.

144. Harwood FL, Amiel D. Differential metabolic responses of periarticular ligaments and tendon to joint immobilization. *J Appl Physiol* 1992;72(5):1687-1691.

145. Eyre DR, Koob TJ, Van Ness KP. Quantitation of hydroxypyridinium crosslinks in collagen by high-performance liquid chromatography. *Analytical Biochemistry* 1984;137(2):380-388.

146. Karlon WJ, McCulloch AD, Covell JW, Hunter JJ, Omens JH. Regional dysfunction correlates with myofiber disarray in transgenic mice with ventricular expression of ras. *Am. J. Physiol. Heart. Circ. Physiol.* 2000;278(3):H898-906.

147. Robinson TF, Cohen-Gould L, Factor SM. Skeletal framework of mammalian heart muscle. Arrangement of inter- and pericellular connective tissue structures. *Lab. Invest.* 1983;49(4):482-498.

148. Omens JH, Miller TR, Covell JW. Relationship between passive tissue strain and collagen uncoiling during healing of infarcted myocardium. *Cardiovasc Res* 1997;33(2):351-358.

149. Bogen DK, Rabinowitz SA, Needleman A, McMahon TA, Abelmann WH. An analysis of the mechanical disadvantage of myocardial infarction in the canine left ventricle. *Circ Res* 1980;47(5):728-741.

150. Ray PS, Martin JL, Swanson EA, Otani H, Dillmann WH, Das DK. Transgene overexpression of {alpha}B crystallin confers simultaneous protection against cardiomyocyte apoptosis and necrosis during myocardial ischemia and reperfusion. *FASEB J.* 2001;15(2):393-402.

151. Ayada Y, Kusachi S, Murakami T, Hirohata S, Takemoto S, Komatsubara I, et al. Increased Expression of Biglycan mRNA in Pressure-Overloaded Rat Heart. *Clin. Exp. Hypertens.* 2001;23(8):633-643.

152. Urbanek K, Torella D, Sheikh F, De Angelis A, Nurzynska D, Silvestri F, et al. Myocardial regeneration by activation of multipotent cardiac stem cells in ischemic heart failure. *Proceedings of the National Academy of Sciences of the United States of America* 2005;102(24):8692-8697.

153. The Jackson Laboratories JAX® Mice Data Sheet, Stock No. 000486.

154. Li X, Gu W, Masinde G, Hamilton-Ulland M, Xu S, Mohan S, et al. Genetic control of the rate of wound healing in mice. *Heredity* 2001;86(6):668-674.

155. Haris Naseem R, Meeson AP, Michael DiMaio J, White MD, Kallhoff J, Humphries C, et al. Reparative myocardial mechanisms in adult C57BL/6 and MRL mice following injury. *Physiol. Genomics* 2007;30(1):44-52.

156. Boyle MP, Weisman HF. Limitation of infarct expansion and ventricular remodeling by late reperfusion. Study of time course and mechanism in a rat model. *Circulation* 1993;88(6):2872-2883.

157. Reffelmann T, Hale SL, Dow JS, Kloner RA. No-Reflow Phenomenon Persists Long-Term After Ischemia/Reperfusion in the Rat and Predicts Infarct Expansion. *Circulation* 2003;108(23):2911-2917.

158. Gentleman R, Carey V, Bates D, Bolstad B, Dettling M, Dudoit S, et al. Bioconductor: open software development for computational biology and bioinformatics. *Genome Biology* 2004;5(10):R80.

159. Wu Z, Irizarry RA. Preprocessing of oligonucleotide array data. *Nat Biotech* 2004;22(6):656-658.

160. Smyth GK. Linear models and empirical bayes methods for assessing differential expression in microarray experiments. *Stat Appl Genet Mol Biol* 2004;3(1):Article 3.

161. van der Laan M, Pollard K. A New Algorithm for Hybrid Hierarchical Clustering with Visualization and the Bootstrap. *Division of Biostatistics, Univ. of California, Berkeley, Technical Report No. 93* 2001.

162. Doniger S, Salomonis N, Dahlquist K, Vranizan K, Lawlor S, Conklin B. MAPPFinder: using Gene Ontology and GenMAPP to create a global gene-expression profile from microarray data. *Genome Biology* 2003;4(1):R7.

163. Ashton KJ, Headrick JP. Quantitative (Real-Time) RT-PCR in Cardiovascular Research. In: Zhang J, Rokosh G, editors. *Cardiac Gene Expression: Methods and Protocols*. Totowa, NJ: Humana Press, 2007:121-143.

164. Au PYB, Martin N, Chau H, Moemeni B, Chia M, Liu F-F, et al. The oncogene PDGF-B provides a key switch from cell death to survival induced by TNF. 2005;24(19):3196-3205.

165. Ugur O, Kathryn AG, Kimberlee D-H, Edward M, William BS. NG2 proteoglycan is expressed exclusively by mural cells during vascular morphogenesis. *Developmental Dynamics* 2001;222(2):218-227.

166. Yang X, Khosravi-Far R, Chang HY, Baltimore D. Daxx, a Novel Fas-Binding Protein That Activates JNK and Apoptosis. *Cell* 1997;89(7):1067-1076.

167. Pattanapanyasat K, Pengruangrojanachai V, Thepthai C, Suwanagool S, Wasi C. Flow cytometric three-color determination of CD4 T-lymphocytes on blood specimens from AIDS patients who have a large number of contaminating non-lymphocytes. *Asian Pac J Allergy Immunol* 1994;12(2):105-9.

168. Askari AT, Brennan M-L, Zhou X, Drinko J, Morehead A, Thomas JD, et al. Myeloperoxidase and Plasminogen Activator Inhibitor 1 Play a Central Role in Ventricular Remodeling after Myocardial Infarction. *J. Exp. Med.* 2003;197(5):615-624.

169. Brunner S, Winogradow J, Huber BC, Zaruba M-M, Fischer R, David R, et al. Erythropoietin administration after myocardial infarction in mice attenuates ischemic cardiomyopathy associated with enhanced homing of bone marrow-derived progenitor cells via the CXCR-4/SDF-1 axis. *FASEB J.* 2009;23(2):351-361.

170. Walz A, Dewald B, von Tscharner V, Baggiolini M. Effects of the neutrophil-activating peptide NAP-2, platelet basic protein, connective tissue-activating peptide III and platelet factor 4 on human neutrophils. *J. Exp. Med.* 1989;170(5):1745-1750.

171. Suzuki K, Murtuza B, Smolenski RT, Sammut IA, Suzuki N, Kaneda Y, et al. Overexpression of Interleukin-1 Receptor Antagonist Provides Cardioprotection Against Ischemia-Reperfusion Injury Associated With Reduction in Apoptosis. *Circulation* 2001;104(90001):I-308-313.

172. Roubille F, Combes S, Leal-Sanchez J, Barrere, Christian, Cransac F, et al. Myocardial Expression of a Dominant-Negative Form of Daxx Decreases Infarct Size and Attenuates Apoptosis in an In Vivo Mouse Model of Ischemia/Reperfusion Injury. *Circulation* 2007;116(23):2709-2717.

173. Cavasin MA, Sankey SS, Yu A-L, Menon S, Yang X-P. Estrogen and testosterone have opposing effects on chronic cardiac remodeling and function in mice with myocardial infarction. *Am J Physiol Heart Circ Physiol* 2003;284(5):H1560-1569.

174. Blankenhorn EP, Troutman S, Clark LD, Zhang X-M, Chen P, Heber-Katz E. Sexually dimorphic genes regulate healing and regeneration in MRL mice. *Mammalian Genome* 2003;14(4):250-260.

175. Cleutjens JP, Verluyten MJ, Smiths JF, Daemen MJ. Collagen remodeling after myocardial infarction in the rat heart. *Am J Pathol* 1995;147(2):325-338.

176. Ross RS, Borg TK. Integrins and the Myocardium. *Circ Res* 2001;88(11):1112-1119.

177. Woodiwiss AJ, Tsotetsi OJ, Sprott S, Lancaster EJ, Mela T, Chung ES, et al. Reduction in Myocardial Collagen Cross-Linking Parallels Left Ventricular Dilatation in Rat Models of Systolic Chamber Dysfunction. *Circulation* 2001;103(1):155-160.

178. Margulies KB, Bednarik DP, Dries DL. Genomics, Transcriptional Profiling, and Heart Failure. *Journal of the American College of Cardiology* 2009;53(19):1752-1759.

179. van den Bosch BJC, Lindsey PJ, van den Burg CMM, van der Vlies SA, Lips DJ, van der Vusse GJ, et al. Early and transient gene expression changes in pressure overload-induced cardiac hypertrophy in mice. *Genomics* 2006;88(4):480-488.

180. Berthiaume J, Wallace K. Persistent Alterations to the Gene Expression Profile of the Heart Subsequent to Chronic Doxorubicin Treatment. *Cardiovascular Toxicology* 2007;7(3):178-191.

181. Thum T, Galuppo P, Wolf C, Fiedler J, Kneitz S, van Laake LW, et al. MicroRNAs in the Human Heart: A Clue to Fetal Gene Reprogramming in Heart Failure. *Circulation* 2007;116(3):258-267.

182. Kittleson MM, Minhas KM, Irizarry RA, Ye SQ, Edness G, Breton E, et al. Gene expression analysis of ischemic and nonischemic cardiomyopathy: shared and distinct genes in the development of heart failure. *Physiol. Genomics* 2005;21(3):299-307.

183. Zambon AC, Zhang L, Minovitsky S, Kanter JR, Prabhakar S, Salomonis N, et al. Gene expression patterns define key transcriptional events in cell-cycle regulation by cAMP and protein kinase A. *Proceedings of the National Academy of Sciences of the United States of America* 2005;102(24):8561-8566.

184. Woo YJ, Panlilio CM, Cheng RK, Liao GP, Atluri P, Hsu VM, et al. Therapeutic Delivery of Cyclin A2 Induces Myocardial Regeneration and Enhances Cardiac Function in Ischemic Heart Failure. *Circulation* 2006;114(1_suppl):I-206-213.